

Review

Heterogeneous Iron-Based Catalysts for Organic Transformation Reactions: A Brief Overview

Manash J. Baruah ^{1,2}, Rupjyoti Dutta ^{3,4}, Magdi E. A. Zaki ⁵ and Kusum K. Bania ^{2,*}¹ Department of Chemistry, DCB Girls' College, Jorhat 785001, Assam, India; manashl@tezu.ernet.in² Department of Chemical Sciences, Tezpur University, Napaam, Tezpur 784028, Assam, India³ CSIR-North East Institute of Science and Technology, Jorhat 785006, Assam, India; rupjyotid@tezu.ernet.in⁴ Academy of Scientific and Innovative Research (AcSIR), Ghaziabad 201002, Uttar Pradesh, India⁵ Department of Chemistry, Imam Mohammad Ibn Saud Islamic University (IMSIU), Riyadh 11623, Saudi Arabia; mezaki@imamu.edu.sa

* Correspondence: kusum@tezu.ernet.in

Abstract: Iron (Fe) is considered to be one of the most significant elements due to its wide applications. Recent years have witnessed a burgeoning interest in Fe catalysis as a sustainable and cost-effective alternative to noble metal catalysis in organic synthesis. The abundance and low toxicity of Fe, coupled with its competitive reactivity and selectivity, underscore its appeal for sustainable synthesis. A lot of catalytic reactions have been performed using heterogeneous catalysts of Fe oxide hybridized with support systems like aluminosilicates, clays, carbonized materials, metal oxides or polymeric matrices. This review provides a comprehensive overview of the latest advancements in Fe-catalyzed organic transformation reactions. Highlighted areas include cross-coupling reactions, C–H activation, asymmetric catalysis, and cascade processes, showcasing the versatility of Fe across a spectrum of synthetic methodologies. Emphasis is placed on mechanistic insights, elucidating the underlying principles governing iron-catalyzed reactions. Challenges and opportunities in the field are discussed, providing a roadmap for future research endeavors. Overall, this review illuminates the transformative potential of Fe catalysis in driving innovation and sustainability in organic chemistry, with implications for drug discovery, materials science, and beyond.

Keywords: heterogeneous; Fe catalyst; magnetic; organic reaction; sustainable chemistry



Citation: Baruah, M.J.; Dutta, R.; Zaki, M.E.A.; Bania, K.K. Heterogeneous Iron-Based Catalysts for Organic Transformation Reactions: A Brief Overview. *Molecules* **2024**, *29*, 3177. <https://doi.org/10.3390/molecules29133177>

Academic Editor: Dingyi Wang

Received: 22 May 2024

Revised: 15 June 2024

Accepted: 19 June 2024

Published: 3 July 2024



Copyright: © 2024 by the authors. Licensee MDPI, Basel, Switzerland. This article is an open access article distributed under the terms and conditions of the Creative Commons Attribution (CC BY) license (<https://creativecommons.org/licenses/by/4.0/>).

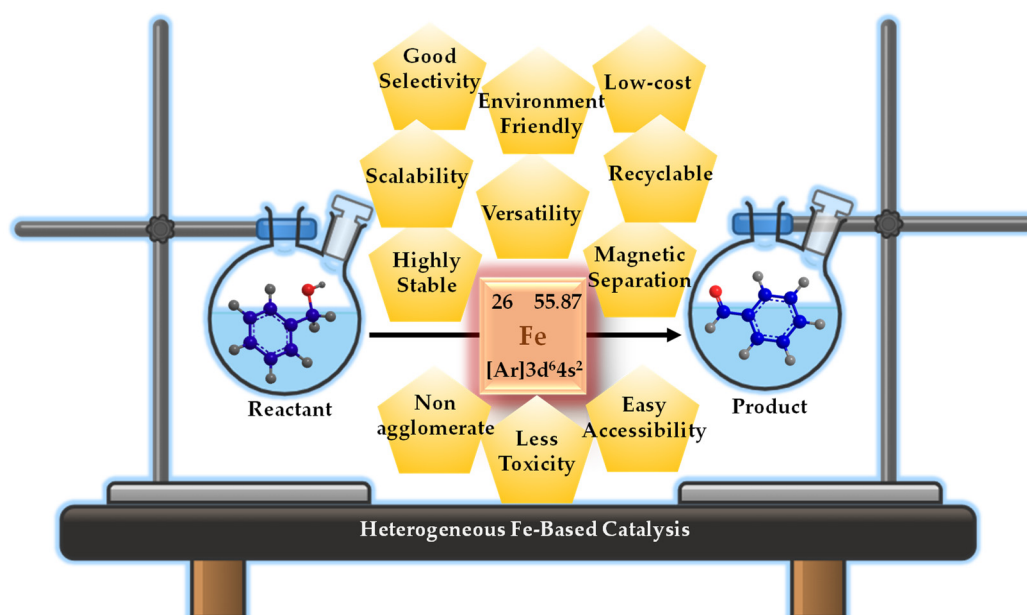
1. Introduction

The synthesis of organic compounds lies at the heart of chemistry, serving as the foundation for advancements in medicine, materials science, and numerous other fields [1,2]. Over the years, scientists have developed a myriad of synthetic methods to construct complex molecules with precision and efficiency [3,4]. Among these methods, catalysis stands out as a powerful strategy, allowing for the selective activation of chemical bonds and the facilitation of otherwise challenging transformations [5,6]. Transition metal catalysis has emerged as a cornerstone of modern synthetic chemistry, enabling a broad range of transformations that were once thought to be impossible or impractical [6,7]. Metals such as palladium (Pd), platinum (Pt), gold (Au), and ruthenium (Ru) have traditionally dominated this field, owing to their ability to catalyze a wide array of reactions with high efficiency and selectivity [6–10]. However, the scarcity and high cost of these noble metals have spurred efforts to develop catalytic systems based on more abundant and inexpensive alternatives.

In recent years, iron (Fe) has emerged as a particularly promising candidate for catalysis, owing to its abundance, low cost, and low toxicity [11,12]. Once considered a stoichiometric reagent or a catalyst for relatively simple reactions, Fe has undergone a renaissance in catalysis, fueled by advances in heterogeneous catalysis, owing to its several advantages [13,14]. The resurgence of heterogeneous Fe catalysis can be attributed to

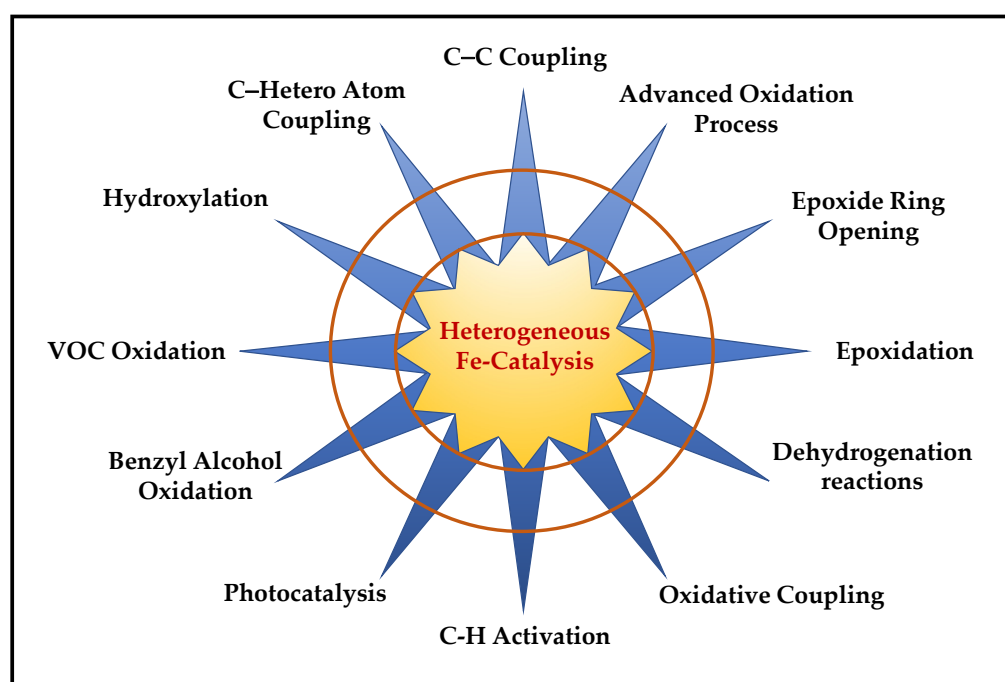
several key factors. Firstly, the desire to reduce the environmental impact of synthetic chemistry has prompted researchers to seek alternatives to precious metal catalysts [12]. Fe, as an Earth-abundant element with low toxicity, represents an attractive candidate for addressing these concerns [11,15]. Additionally, advances in catalyst design and reaction engineering have led to the development of heterogeneous Fe catalysts with improved activity, selectivity, and stability, enabling the synthesis of a wide range of organic compounds under mild conditions [16]. This potential has led to a wave of chemical research focused on harnessing the catalytic potential of Fe for a diverse array of organic transformations [12,14].

Heterogeneous Fe-based catalysts offer several advantages: Scheme 1 [16,17]. Apart from the cost-effective and environmentally friendly nature, they can be easily separated from reaction mixtures, facilitating catalyst recovery and reuse [16]. These catalysts typically exhibit high stability and durability under reaction conditions. They exhibit high thermal and chemical stability, making them suitable for a wide range of reaction conditions [18]. These catalysts often simplify purification processes by reducing product contamination with catalyst residues. Additionally, heterogeneous Fe catalysts can be engineered for high selectivity in specific reactions [14]. Their robustness and ease of handling make them advantageous for large-scale industrial processes [13]. Capable of catalyzing a broad spectrum of organic transformation reactions, these catalysts also limit side reactions within their confined environment, thereby improving overall yield and efficiency [17]. Moreover, magnetic nanoparticles (NPs) offer significant potential in heterogeneous catalysis due to their easy separation and reusability [19]. Their saturation magnetization depends on size and surface properties, with small nanoparticles prone to aggregation [20]. Coating them with materials like silica, carbon, metals, metal oxides, or polymers prevents aggregation and enhances catalytic activity by supporting active species on their high surface area [21]. The field of heterogeneous Fe-catalyzed organic transformation reactions has been expanding rapidly in the last several years [16,17]. A broad range of organic reactions, including hydrogenation, oxidation, activation, coupling, and cycloaddition processes, have been described in the literature [16,17]. These reactions involve a wide range of bond formations, including aryl–aryl, aryl–alkyl, alkyl–alkyl, and heteroatom cross-couplings, among others [16,17]. Moreover, heterogeneous Fe catalysts have been shown to exhibit high functional group tolerance, allowing for the direct coupling of substrates bearing a variety of functional groups without the need for pre-activation or protection strategies [22]. One of the most significant areas of progress in heterogeneous Fe catalysis lies in cross-coupling reactions, a class of transformations that are widely used in organic synthesis for the formation of carbon–carbon and carbon–heteroatom bonds [17,22]. Usually, cross-couplings have been dominated by Pd and other precious metals, which offer high reactivity and selectivity but are limited by their scarcity and high cost [23]. In recent years, however, heterogeneous Fe catalysts have emerged as viable alternatives for cross-coupling reactions, offering competitive reactivity and selectivity profiles while addressing the limitations of precious metal catalysts [22]. In addition to cross-coupling reactions, heterogeneous Fe catalysis has found applications in a variety of other synthetic transformations. For example, Fe-catalyzed C–H activation and functionalization reactions have emerged as powerful tools for the direct functionalization of C–H bonds, enabling the synthesis of complex molecules with high efficiency and selectivity [24]. Similarly, heterogeneous Fe catalysts have been employed in asymmetric transformations, providing access to enantioenriched compounds with high levels of stereo control [25]. Additionally, Fe catalysts have been used in cascade reactions, in which multiple bond-forming events occur sequentially in a single reaction vessel, leading to the rapid synthesis of complex molecular architectures [26]. Recent advancements highlight the diverse applications of magnetic nanomaterials in catalysis, including hydrogenation, Suzuki–Miyaura coupling, oxidation, chiral catalysis, enzyme catalysis, photocatalysis, electrocatalysis, and photoelectrochemical catalysis [17,27].



Scheme 1. Advantages of heterogeneous Fe-based catalysts in organic transformation reactions.

In this article, we will provide a comprehensive overview of the recent advances in heterogeneous Fe-catalyzed organic transformation reactions. A brief exploration will be performed in this article within the time period 2019–2024, including the application of heterogeneous Fe catalysis in a variety of synthetic transformations, together with cross-coupling reactions, C–H activation, coupling reactions, oxidation, hydroxylation reactions, etc. (Scheme 2). Finally, we will discuss the current challenges and future directions in the field, highlighting opportunities for further innovation and development. Through this brief review, we expect to provide insights into the transformative potential of heterogeneous Fe catalysis and inspire further research in this exciting and rapidly evolving area of chemistry.

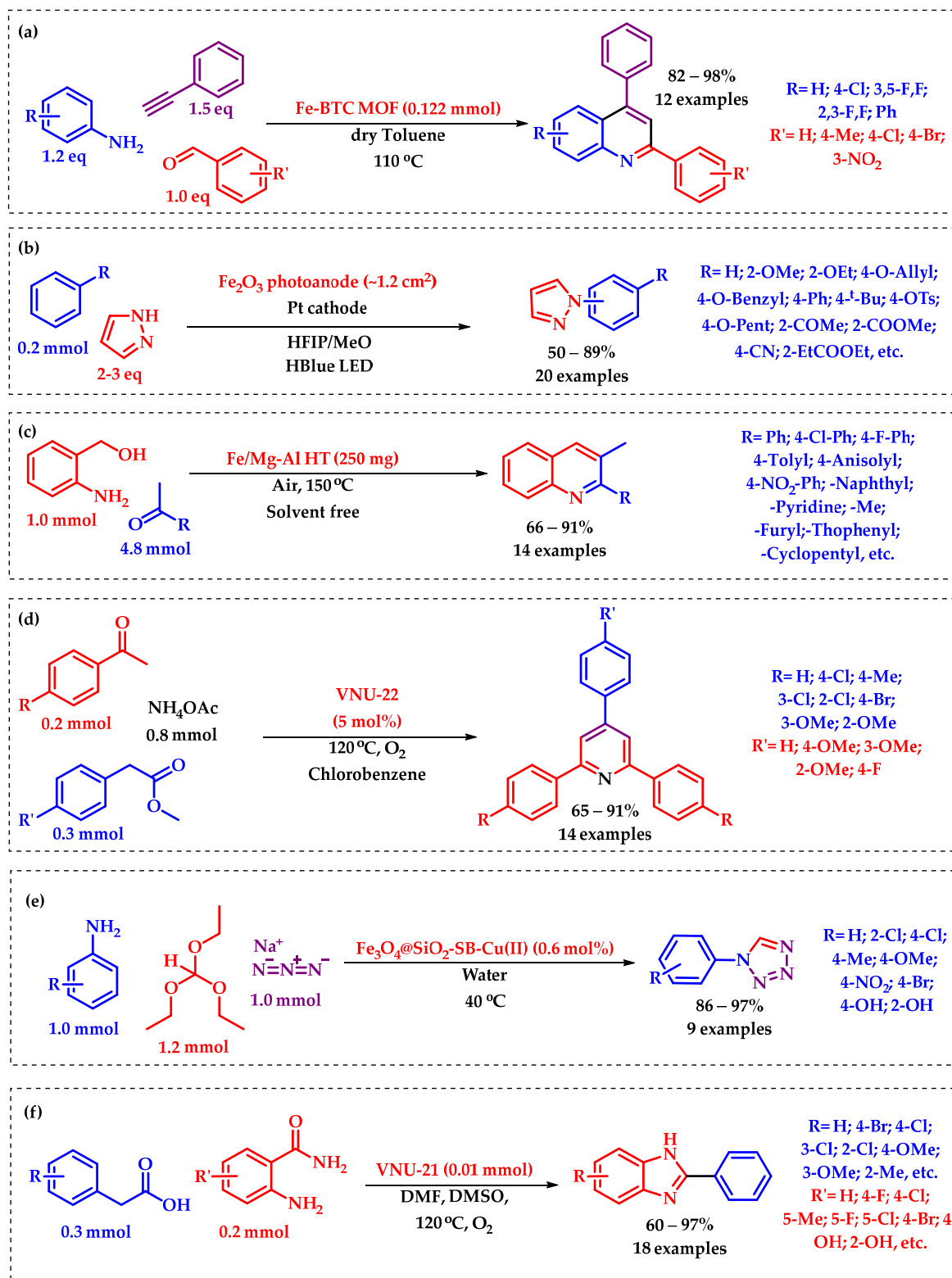


Scheme 2. Perspectives of Fe-catalyzed organic reactions.

2. C–H Activation Reaction

C–H activation is a chemical process where a C–H bond within an organic molecule is cleaved or 'activated' to form new bonds, typically involving the introduction of functional groups [28,29]. This reaction is significant in synthetic chemistry as it allows for the direct transformation of simple and abundant hydrocarbons into more complex and valuable molecules without the need for pre-functionalization [30,31]. C–H activation reactions often require transition metal catalysts to facilitate the bond cleavage and subsequent functionalization steps [32]. These reactions have broad applications in the synthesis of pharmaceuticals, agrochemicals, materials, and fine chemicals, offering efficient routes to structurally diverse compounds [33–35]. Research shows that a good number of heterogeneous Fe catalysts have been employed in various C–H activation reactions, including cross-coupling, cyclization, and functionalization reactions, contributing significantly to the development of sustainable synthetic methodologies [36–38]. E. Nakamura is regarded as a pioneer in the field of C–H activation reactions. He and his research group have previously shown a comprehensive analysis of previous studies on C–H activation processes catalyzed by Fe [39]. His research showcased the activation of C–H bonds and subsequent reactions with alkynes to form cyclized products [40,41]. Nakamura's achievements include the direct phenylation of isoxazoles using palladium and the methylation of naphthylamide with iron catalysts [42]. These works have broadened the scope of C–H activation, emphasizing the use of economical and less toxic metals like iron in these chemical processes [43]. However, it is noteworthy to mention herein that Lutz Ackermann is a well-known chemist who has made significant contributions to the field of C–H activation [44–46]. Ackermann's work in this area has focused on developing new catalysts and methodologies to facilitate these transformations with greater efficiency and selectivity [47–49]. In addition to Ackermann's contributions, Professor G. Cera and S. Cattani have also reviewed recent advancements in iron-catalyzed C–H activation reactions, particularly focusing on synthetic chemistry applications [50]. Very recently, Lemmens et al. derived an Fe-based metal–organic framework (MOF), CAU-27-Fe as a suitable heterogeneous catalyst for C–H activation reaction [33]. The CAU-27-Fe was utilized for direct C–H amination of ether by N-heterocycles under mild reaction conditions. This highly stable catalyst was reported to be reused for multiple runs, making it an efficient and sustainable option for novel C–H activation processes. The discussed protocol is particularly suitable for the synthesis of key pharmaceutical precursors, enhancing its relevance in the field of drug development. Zhang et al. developed a photo-electrocatalytic methodology for C–H amination of arene using robust and earth-abundant hematite (α -Fe₂O₃) as the catalyst [51]. This technique enabled the preparation of various heterocycles with aryl C–N moieties from simple arenes and azoles without looking for pre-functionalization. The reported approach could be successfully applied to the functionalization of several pharmaceutical molecules, pioneering the use of photoelectrochemical cells in organic synthesis. Recently, Devaranjan and Suresh developed an Fe-based sustainable heterogeneous MOF catalyst, Fe(BTC), which was proven to be highly effective for synthesizing 2,4-diarylquinolines [52]. This reported method avoided the need for stoichiometric amounts of catalyst and sensitive reagents, producing 2,4-diarylquinolines in good to excellent yields with broad functional group tolerance. This MOF was found to be easily separated by filtration and reused over five times without significant loss of activity. In another work, To et al. synthesized one more Fe-MOF (VNU-21) using 1,3,5-benzenetricarboxylic acid (BTC), 4,4'-ethynylenedibenzoic acid, and FeCl₂ for the one-pot synthesis of quinazolinones [53]. In this procedure, Fe-catalyzed oxidative Csp³–H bond activation was used to decarboxylate phenylacetic acids, followed by the metal-free oxidative cyclization using 2-aminobenzamides. Additionally, the catalyst was found to be recycled up to a good number of catalytic cycles without experiencing a discernible decrease in performance. Again, a new Fe-MOF, VNU-22 {[Fe₃(BTC)(BPDC)₂·11.97H₂O]}, was synthesized by Doan et al., using BTC³⁻ (1,3,5-benzenetricarboxylate), BPDC²⁻ (4,4'-biphenyldicarboxylate), and an Fe–carbonyl complex [Fe₃(CO)₂]₇ [54]. The VNU-22 was reported to efficiently catalyzed

the synthesis of 2,4,6-triphenylpyridines from acetophenones, phenylacetic acids, and ammonium acetate through the C–H activation process. The MOF was easily recovered and reused without significant loss of catalytic performance, representing an industrially attractive synthetic pathway.



Scheme 3. (a) [52], (b) [51], (c) [55], (d) [54], (e) [56], and (f) [53]. Some significant reported outcomes of heterogeneous Fe-catalyzed C–H activation reactions.

Recently, Waghchaure et al. derived a superior heterogeneous catalyst of Fe doped ZnO (Fe-ZnO) for Biginelli reaction for the production of 3,4-dihydropyrimidin-2-one derivatives [57]. Using a one-pot, three-component reaction with urea, a β -dicarbonyl compound, and various aromatic aldehydes, a minimal amount of the Fe-ZnO catalyst was reported to be efficiently synthesized 3,4-dihydropyrimidinones. Furthermore, this protocol offered advantages such as short reaction time, high product purity, catalyst recyclability and reusability. A bifunctional heterogeneous catalyst, based on Mg-Al hydrotalcite, was designed by Motokura et al. in porous FeO(OH) to facilitate the one-pot synthesis of 2-substituted quinoline derivatives via dehydrogenative oxidation-cyclization processes [55]. Without the need for extra homogenous bases or solvents, this reported protocol proceeded well in an open atmosphere under cost-effective Fe catalysis. Julián E. Sánchez-Velandia and Aída Luz Villa designed Fe(III)-based heterogeneous catalysts supported on MCM-41 for α - and β -pinene epoxide isomerization [58]. The synthesized catalyst exhibited excellent productivity for the α -pinene epoxide isomerization reaction with a high turnover number (TON) of 364 along with greater % conversion (73%) and selectivity (59%) towards the formation of campholenic aldehyde. For β -pinene epoxide, the catalyst had the highest TON of 299 with a 60% conversion and 100% selectivity to myrtanal. The activity of the catalyst was also correlated with metal oxides, particle diameter, as well as acidity strength. However, the catalyst maintained its heterogeneity over five cycles with moderate to good activity. A new environmentally friendly Silica coated (SiO₂) Fe-oxide-based heterogeneous catalyst, Fe₃O₄@SiO₂-Im(Br)-SB-Cu(II), was synthesized by Mashhoori and Sandaroos, and utilized for generating tetrazole derivatives in water media [56]. The reported catalyst showed exceptional efficiency with 97% yield of tetrazole. The catalyst's efficacy was also studied and was credited to the combined action of the Fe-center and the imidazolium ion. Additionally, it could be reused for several catalytic cycles without significant loss in catalytic activity and without causing contamination. Scheme 3 demonstrates some interesting heterogeneous Fe-catalyzed C–H activation processes.

3. C–C Coupling Reactions

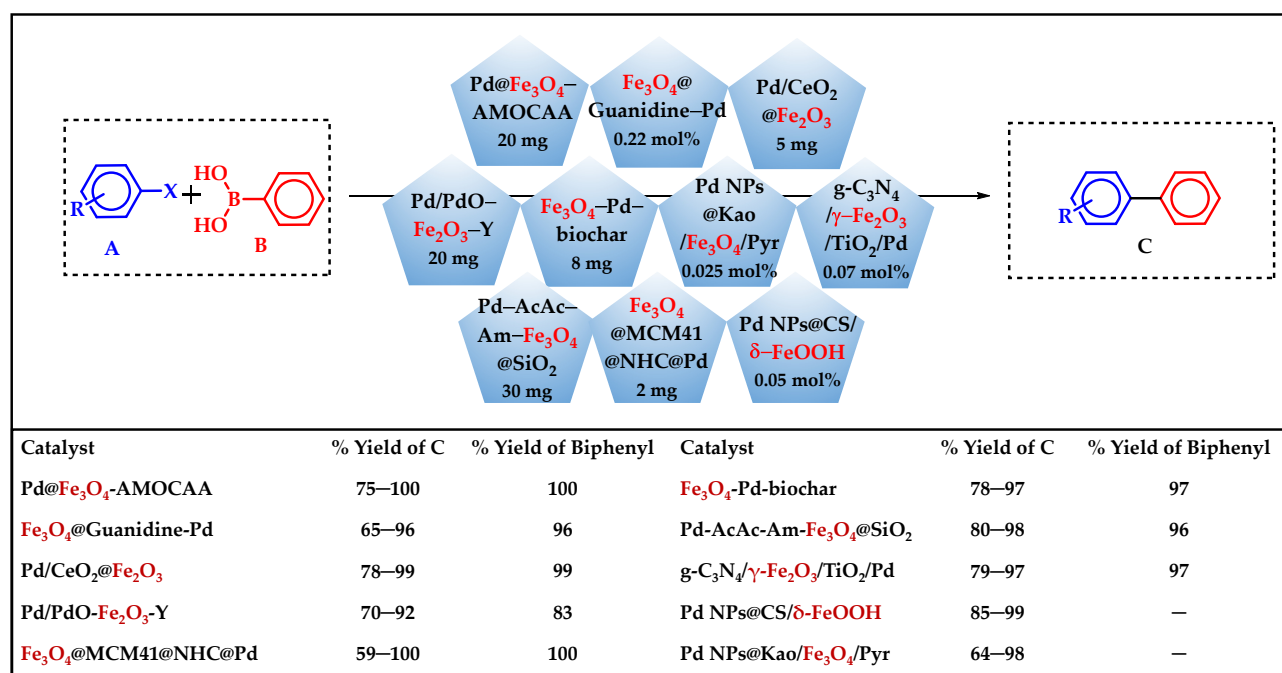
C–C coupling reactions catalyzed by heterogeneous Fe represent a transformative approach in organic synthesis, harnessing the abundance, low cost, and eco-friendliness of Fe as a transition metal catalyst [59,60]. These reactions involve the formation of C–C bonds between two or more organic substrates, enabling the construction of complex molecular architectures with high efficiency and selectivity [60]. The field of C–C coupling reactions has witnessed remarkable advancements with Fe catalysts, showcasing their versatility across a spectrum of synthetic methodologies [59]. From traditional cross-coupling reactions to novel transformations like direct C–H functionalization, Fe catalysis has emerged as a powerful tool for chemists seeking sustainable and economical routes to intricate molecular structures [59,60]. Moreover, the development of ligands and reaction conditions tailored to Fe catalysis has expanded the scope of these transformations, allowing access to previously inaccessible chemical space [61]. In addition to fundamental advancements, recent years have witnessed the application of Fe-catalyzed C–C coupling reactions in the synthesis of complex natural products, pharmaceuticals, and functional materials [28]. These transformative achievements highlight the practical significance of Fe catalysis in addressing societal needs and advancing drug discovery, materials science, and sustainable chemistry. Recently, Jang et al. conducted an in-depth analysis on hybrid Pd–Fe₃O₄ nanocatalysts, with specific attention given to urchin-like FePd–Fe₃O₄, Pd/Fe₃O₄, Pd/Fe₃O₄/charcoal, as well as flower-like Pd–Fe₃O₄ nanocomposites [62]. These nanocomposites are utilized as effective catalysts for various C–C coupling reactions, such as Suzuki-Miyaura (SM), Heck, and Sonogashira reactions, showcasing superior catalytic activity and reusability compared to many previously reported catalysts, owing to their magnetic properties. Due to their well-organized morphology and magnetic characteristics these hybrid Fe-based nanostructures give outstanding performance in terms of product yield, stability of the catalyst, and recyclability. Similarly, Hegde et al. designed a Pd functionalized nanocatalyst

using silica-coated Fe-oxide and furaldehyde (FA) Schiff base as a supported material ($\text{Fe}_3\text{O}_4@\text{SiO}_2\text{-FA-Pd}$) [63]. Using the synthesized $\text{Fe}_3\text{O}_4@\text{SiO}_2\text{-FA-Pd}$ NPs as a magnetic nanocatalyst, the Mizoroki–Heck reaction of arylbromide and terminal alkenes resulted in effective reactivity with excellent yields. Very recently, Sonawane et al. developed a silica-supported Fe-oxide-based catalyst, Pd-SILP- $\text{Fe}_3\text{O}_4@\text{SiO}_2$, for Sonogashira coupling in aqueous media under aerobic conditions [64]. The synthesized nanocatalyst demonstrated excellent thermal stability, high catalytic efficiency, elevated turnover frequencies (TOFs), simple magnetic recovery, high recyclability, compatibility with aqueous systems, and thereby facilitating the reactions using water as a green solvent. Sardarian et al. developed a new Fe-oxide-based organometallic catalyst by binding Pd(0) to polyvinyl alcohol-modified $\text{Fe}_3\text{O}_4@\text{SiO}_2$ nanospheres, designated as $\text{Fe}_3\text{O}_4@\text{SiO}_2\text{-PVA-Pd(0)}$ [65]. The system employed in Heck and Sonogashira coupling reactions in aqueous environments. Interestingly, it demonstrated outstanding performance with minimal Pd content, yielding excellent product yield and attaining high TOFs. Additionally, the catalysts behaved as magnetically retrievable with high recyclability rates. Again, a biochar-based nanocomposite catalyst was developed by Akay et al. by sequentially depositing Fe_3O_4 and Pd onto a biochar surface derived from waste biomass [66]. The Pd- Fe_3O_4 biochar catalyst exhibited high catalytic efficiency for the SM coupling reaction across various experimental conditions, bases, and aryl halides. It achieved an optimal yield of 99% in the coupling reaction between aryl iodide and phenylboronic acid using only 8 mg of catalyst, K_2CO_3 as the base, and in a solvent-free setup with microwave irradiation. The catalyst's broader applicability to SM coupling reactions was demonstrated with a variety of aryl chlorides, bromides, and iodides. Moreover, the catalyst maintained consistent activity over eight consecutive runs, underscoring its potential for recovery and reuse. To perform SM and Sonogashira coupling reactions, Tamoradi et al. designed a bifunctional reusable Fe-oxide-based catalyst (Pd@ Fe_3O_4 /AMOCOA) by complexing Pd with magnetic Fe_3O_4 nanoparticles coated with a 2-(7-amino-4-methyl-2-oxo-2H-chromen-3-yl)acetic acid (AMOCOA) [67]. The advantages of the system include the use of non-toxic, commercially available, or easily accessible starting materials for the synthesis of the catalyst, straightforward recovery, high product yields in short reaction times, operational simplicity, robust activity, and stability, making it highly suitable for industrial and pharmaceutical applications. Similarly, Halligudra et al. introduced an $\text{Fe}_3\text{O}_4@\text{Guanidine-Pd}$ nanocatalyst effective for SM cross-coupling of aryl halides with phenylboronic acids and for selectively reducing nitroarenes to their corresponding amines [68]. The prepared $\text{Fe}_3\text{O}_4@\text{Guanidine-Pd}$ demonstrated efficient catalytic performance by achieving conversion of aryl halides to biaryl derivatives in aqueous medium with minimal catalyst (0.22 mol %) and shorter reaction time while maintaining high TON and TOFs. Notably, the synthesized $\text{Fe}_3\text{O}_4@\text{Guanidine-Pd}$ was reported to be magnetically separable, with a very high recyclability rate without significant loss of catalytic activity. Recently, Bora et al. designed a novel nanocatalyst consisting of Pd/PdO and Fe_2O_3 NPs, zeolite-Y support, and Pd/PdO- $\text{Fe}_2\text{O}_3\text{-Y}$ [69]. The catalyst was reported to be effective for C–Cl bond activation in aryl chlorides for SM cross-coupling, achieving high yields (up to 92%) with very low Pd loading (0.0037 mol %). The catalyst exhibited excellent thermal stability, and high recyclability. The outstanding productivity of the synthesized nanocatalyst was attributed to the participation of surface hydroxyl groups and modification of basic sites in zeolite-Y. Akkoc et al. developed an $\text{Fe}_3\text{O}_4@\text{MCM-41}@\text{NHC}@\text{Pd}$ catalyst, formed by attaching Pd metal to the N-heterocyclic carbene (NHC) ligand on $\text{Fe}_3\text{O}_4@\text{MCM-41}$, which showed excellent catalytic activity in SM reactions [70]. With just 2 mg of catalyst, it achieved high TOF (up to $408,404\text{ h}^{-1}$) at room temperature in 2-propanol/ H_2O (1:2) solvent media. Similar to the above cited reports, the catalyst could be easily recovered and reused multiple times without notable performance loss, indicating excellent structural and chemical stability. Çalışkan et al. synthesized an Fe-oxide ($\delta\text{-FeOOH}$)-based Pd nanocatalyst (Pd NPs@CS/ $\delta\text{-FeOOH}$) attached to chitosan and utilized this in synthesizing biaryls via an SM reaction with satisfactory yields [71]. Moreover, the catalyst maintained its activity over eight cycles, indicating its potential for

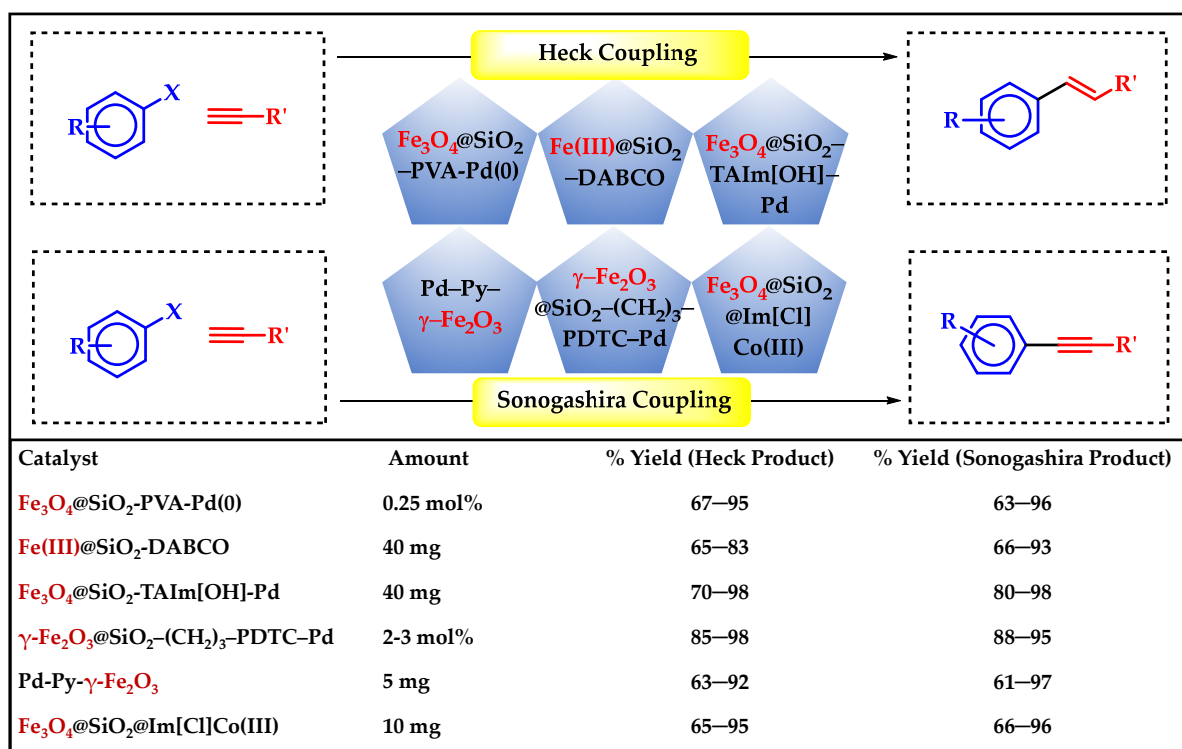
use in diverse organic reactions due to its promising performance and reusability. Recently, Sheikh et al. developed a recyclable magnetic nano Pd-complex, having Fe₂O₃ NPs, which exhibited high efficiency as a catalyst for SM and Mizoroki–Heck coupling reactions [72]. Remarkably, the catalyst displayed high activity in water at moderate reaction conditions (90 °C), with a reasonable reusability rate. Vibhute et al. designed an Fe-oxide-based novel nanomagnetic catalyst (Pd-AcAc-Am-Fe₃O₄@SiO₂) containing Pd over SiO₂ support [73]. The system demonstrated notable efficacy in catalyzing SM cross-coupling reactions of aryl halides with phenylboronic acid. Its performance was evaluated under different conditions, showing excellent yields, mild reaction conditions, short reaction times, and easy magnetic work-up. It exhibited recyclability over at least six cycles without significant loss of activity, making it a promising candidate for sustainable catalysis. A new Fe-based heterogeneous catalyst (Pd NPs@Kao/Fe₃O₄/Pyr) was established by Baran et al. by anchoring Pd NPs onto Fe₃O₄-loaded Schiff-base-modified kaolin [74]. The nanostructure was found to be suitable for SM cross-coupling reactions with high activity across various aryl halides with different functional groups. Additionally, it displayed excellent recyclability, maintaining an 89% yield even after 10 consecutive runs. On the other hand, the photocatalyzed C–C coupling process has been a thriving area of research and development in organic synthesis chemistry and photocatalysis in recent years, offering a promising new approach to C–C bond fabrication. Giving importance to light energy, Liu et al. designed Pd/CeO₂@Fe₂O₃ heterojunctions as an efficient photocatalyst for an SM reaction using solar energy at room temperature [75]. This structure of the material was reported to be layered double hydroxide (LDH), which facilitated light absorption and exposed more active sites (Pd). The resulting abundant oxygen vacancies and Pd/CeO₂@Fe₂O₃ heterojunctions extended the response region of visible light and aided in electron–hole pair separation. The directional transfer of electrons from Fe to Pd accelerated oxidative addition in the SM reactions, leading to high catalytic activity. The catalyst achieved a TOF of 1770 h^{−1} under visible light. Jahanshahi et al. synthesized an Fe-based magnetic nanocomposite, g-C₃N₄/γ-Fe₂O₃/TiO₂/Pd, synthesized as a visible-light photocatalyst, efficiently catalyzed Hiyama and SM cross-coupling reactions, including some challenging aryl chlorides [76]. The catalyst was found to be operative effectively at room temperature under visible light irradiation. As usual, the material could be magnetically separated and reused for up to seven cycles without significant loss of activity. Adam et al. designed Fe₃O₄-supported Cu(II) catalysts immobilized on TiO₂-coated Fe₃O₄ nanoparticles (CuL@TiO₂@Fe₃O₄, where L is tridentate iminoisonicotine ligand) [77]. The catalyst was tested in SM coupling and Buchwald–Hartwig (BH) cross-coupling reactions and had an excellent catalytic performance. The reusability test of the catalyst exhibited very good outcomes with high reusability rates. From these scientific analyses, we noticed that magnetic Fe-based materials present a promising additive to Pd catalysts in SM coupling reactions, offering advantages in terms of cost, environmental impact, and ease of recovery (Scheme 4). Continued research into optimizing these systems and understanding their mechanisms will further enhance their applicability and efficiency in organic synthesis.

Nevertheless, while most reports designate Pd as the primary metal for such coupling reactions, there are also some reports discussing Pd-free Heck coupling reactions. Deepa et al. established a chloroglycine–ionic liquid imidazolium supported Fe³⁺ complex as an effective and green catalyst for the Heck reaction [78]. The remarkable features of this catalyst system include the achievement of excellent yields of trans-stilbenes (up to 94%) with just 0.005 mol % of catalyst, and the ability for the catalyst to be readily recovered and reused without significant loss of activity. Similarly, Hajipour et al. reported an Fe-catalyst, Fe(III)@SiO₂-DABCO, for the cross-coupling of aryl iodides, providing a mild basic environment (K₂CO₃ as the base) [79]. The system enables Heck reactions under mild conditions (Pd-free, H₂O solvent, 80 °C, short reaction time). The iron catalyst is highly active and recyclable by simple filtration, offering an economical approach. Its use instead of palladium or copper enhances environmental, economic, and industrial benefits. Additionally, the system facilitates Fe-catalyzed Sonogashira and Heck reactions, expanding

its utility in organic syntheses. Similarly, Min et al. developed a versatile and recyclable magnetite and NHC ligand-based catalyst, $\text{Fe}_3\text{O}_4@\text{SiO}_2\text{-TAIM}[\text{OH}]\text{-Pd}$ for the efficient Heck, Suzuki, and Sonogashira cross-coupling reactions under mild conditions [80]. The NHC ligand precursor was immobilized on magnetite, and its catalytic activity was assessed in these coupling reactions as a heterogeneous catalyst. Again, Sobhani et al. synthesized a novel immobilized Pd-pyridine (Py) complex on $\gamma\text{-Fe}_2\text{O}_3$ magnetic nanoparticles, i.e., $\text{Pd-Py-}\gamma\text{-Fe}_2\text{O}_3$ [81]. The catalytic activity of this synthesized catalyst was examined in Heck, Suzuki, and Sonogashira coupling reactions with various aryl halides. The catalyst could be easily separated from the reaction mixture using an external magnetic field and reused multiple times without significant loss of catalytic activity. Another SiO_2 supported Fe-oxide-based catalyst was also reported by Tashrifi et al., and involved the preparation of a Pd complex of (pyridin-2-ylmethyl)dithiocarbamate (PDTC) supported on $\gamma\text{-Fe}_2\text{O}_3@\text{SiO}_2$ nanoparticles, i.e., $\gamma\text{-Fe}_2\text{O}_3@\text{SiO}_2\text{-(CH}_2\text{)}_3\text{-PDTC-Pd}$ [82]. The catalytic performance of this nanomaterial was assessed in Heck and Sonogashira coupling reactions between various aryl halides and different alkenes or phenylacetylene in water. The synthesized nanocatalyst demonstrated high catalytic activity even in very small quantities (<0.1 mol %), and could be reused for ten successive catalytic cycles without any significant activity loss. Similar to the above report, another Fe-oxide-based magnetic catalytic system has been developed by Kazemnejadi et al. for Heck and Sonogashira cross-coupling reactions by decorating the Schiff base Co(III) complex on $\text{Fe}_3\text{O}_4@\text{SiO}_2$ nanoparticles, designated as $\text{Fe}_3\text{O}_4@\text{SiO}_2@\text{Im}[\text{Cl}]\text{Co(III)-melamine nanocomposite}$ [83]. The catalyst demonstrated compatibility with a variety of substrates, achieving high to excellent yields for both Heck and Sonogashira coupling products. Additionally, the catalyst proved its true heterogeneity by empowering its recyclability rate up to the seventh consecutive run. The reactions were conducted using ethanol as the solvent and under base-free conditions, making them suitable from a green and sustainable chemistry perspective. Scheme 5 depicts some of the recently reported Fe-based interesting bifunctional catalytic systems for Heck and Sonogashira coupling reactions.



Scheme 4. Recently reported Fe-oxide based magnetic heterogeneous catalysts for SM coupling reactions.



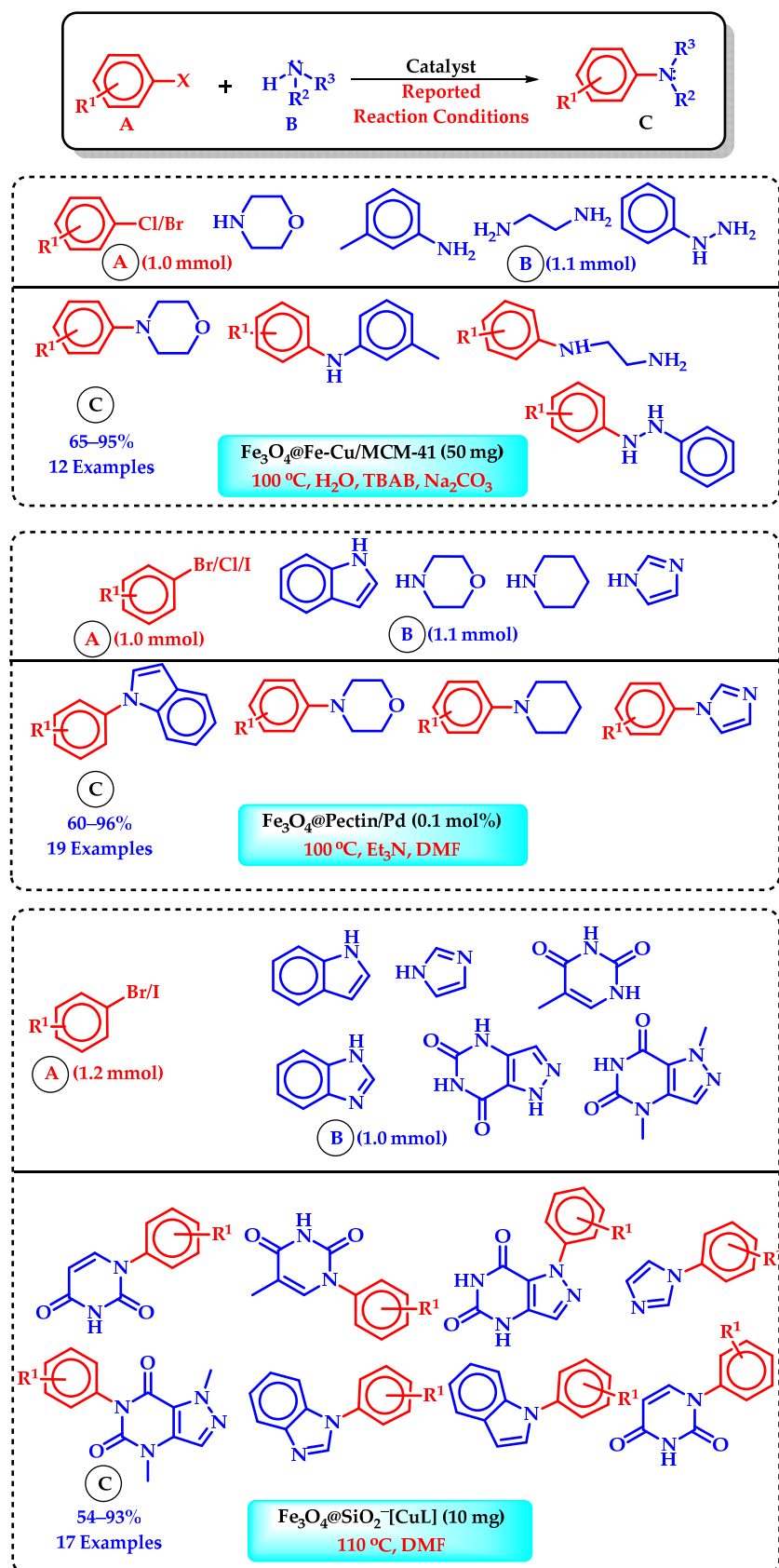
Scheme 5. Some recently reported Fe-oxide based bifunctional catalysts for Heck and Sonogashira coupling reactions [65,79–83].

4. C–N Bond Formation Reactions

The presence of carbon–heteroatom (basically O, N, S) bonds is common in many natural products, medicines, and insecticides [84]. The creation of carbon–heteroatom bonds has, therefore, received a lot of focus for the conception of easy and efficient procedures. Transition-metal-catalyzed cross-coupling reactions represent a promising area of modern organic synthesis, offering efficient and sustainable methods for the construction of carbon–heteroatom bonds [85]. Due to its uniqueness, iron catalysis has consistently been a favored option for such reactions. [12]. The Fe catalyst, a first-row transition metal, typically facilitates cross-coupling reactions by means of a single-electron transfer (SET) process. There are only a handful of reported cases where a two-electron transfer process was involved, demonstrating a distinct reactivity with second- and third-row transition metals, which consistently boost cross-coupling reactions through means of a two-electron transfer process [86]. The production of carbon–heteroatom bonds has lagged behind that of carbon–carbon bonds, despite the abundance of research on carbon–carbon bonding via Fe catalysis [12]. The transition-metal-catalyzed formation of C–N bonds stands out as a pivotal process in organic synthesis, finding widespread application across chemical, pharmaceutical, and materials industries [87]. Traditionally, the BH amination reaction has been the go-to method for accessing C–N bonds, involving the cross-coupling of aryl or alkenyl halides with amines. However, recent years have seen significant advancements in the direct formation of C–N bonds via C–H activation [88]. Despite substantial progress achieved with transition metals such as Cu, Pd, Ni, Fe, and Co, Fe-catalyzed C–N bond formation has received relatively less attention, possibly due to concerns regarding the adverse effects of trace metals. Going through the most recent literature, it was noticed that a lot of research groups presented a good number of results regarding BH amination reactions (Scheme 6). Chahkamali et al. demonstrated an Fe_2O_3 -supported Pd–N-heterocyclic carbene complex for fluoride-free Hiyama, SM, and cyanation (C–N coupling) reactions in pure water [89]. This catalyst effectively yielded various biaryls and aryl nitriles from aryl halides with triethoxyphenylsilane, phenylboronic acid, and $\text{K}_4[\text{Fe}(\text{CN})_6]\cdot 3\text{H}_2\text{O}$. The

presence of sulfonate groups on the catalyst's surface enhanced its water dispersibility and magnetic recoverability. Similarly, an MCM-supported Fe_3O_4 -based nanostructured catalyst, $\text{Fe}_3\text{O}_4@ \text{Fe-Cu/MCM-41}$, was prepared by Abdollahi-Alibeik et al. for BH C–N cross-coupling reaction [90]. Owing to its magnetic behavior, the catalyst demonstrated excellent recoverability and reusability without significant loss of activity or magnetic properties.

Very recently, Amali et al. developed a heterogeneous magnetic nanocatalyst by immobilizing Co NPs onto hollow Fe_3O_4 nanospheres that are covered with a porous covalent triazine framework, $\text{Co/Fe}_3\text{O}_4@ \text{triazine}$ [91]. This magnetically separable catalyst obtained from this process demonstrated exceptional performance in ligand-free BH N-arylation reaction. The nitrogen-enriched porosity structure of the nanocatalyst enhanced the ability to interact with active centers, kept the Co nanoparticles apart to preserve their activity, and prevented them from clumping together during reactions. This guaranteed the stability of the catalytic sites, enabling their reuse without experiencing any decrease in activity. Zhang et al. developed an innovative pectin-functionalized magnetic Fe_3O_4 nanoparticle incorporating Pd ($\text{Fe}_3\text{O}_4@ \text{Pectin/Pd}$) as a heterogeneous nanocatalyst for Suzuki and BH cross-coupling reactions [92]. Owing to its excellent effectiveness, environmental friendliness, and reusability, various biphenyl and arylamine derivatives were efficiently produced. Additionally, the catalyst's performance was maintained over multiple recycling cycles. Recently, Rouzifar et al. derived an innovative multifunctional catalyst containing Fe-MOF functionalized with a Co complex ($\text{Fe-MIL-101-isatin-SB-Co}$) [93]. This modified MOF serves as an efficient heterogeneous and recyclable catalyst for Ullmann, BH, Hirao, Hiyama, and Mizoroki–Heck cross-coupling reactions involving various aryl halides, phenylboronic acid, and phenyl tosylate with phenols, anilines, heterocyclic amines, triethyl phosphite, tri-ethoxyphenylsilane, and alkenes, yielding the desired coupling products in moderate to high yields. Dubey et al. proposed a Pd-doped Fe_3O_4 nanocatalyst with a polydopamine (PDA) coating ($\text{Pd/Fe}_3\text{O}_4@ \text{PDA}$) as an efficient catalyst for the Ullmann homocoupling of various aryl halides, arylboronic acids, and aryl diazonium salts in aqueous media with RM- β -CD [94]. The catalyst was magnetically recoverable and reusable for up to five cycles without significant loss of catalytic activity. To the best of our knowledge, this was the first report of a magnetically recoverable catalyst used for Ullmann homocoupling of these substrates in water. Mansoori et al. synthesized a new bis(NHC)-Pd(II) catalyst supported on magnetic $\text{Fe}_3\text{O}_4@ \text{SBA-15}$ [95]. The material was further immobilized with $\text{trans-[Pd(Cl)}_2(\text{SMe}_2)_2]$ complex to form $\text{Fe}_3\text{O}_4@ \text{SBA-AP-CC-bis(NHC)-Pd(II)}$. This supported Pd(II) complex was reported to efficiently catalyze the direct monoarylation of ammonia with iodo-, bromo-, and chloroarenes with greater selectivity. Similar to the previous reports, the catalyst could be magnetically separable and reusable for several cycles with minimal deactivation. Hemmati et al. reported a novel magnetic Fe-oxide-based nanocatalyst ($\text{Fe}_3\text{O}_4@ \text{PVA/CuCl}$) with an Fe_3O_4 NP coating of with polyvinyl alcohol (PVA) followed by coordination with CuCl [96]. The reported material exhibited high efficiency in the N-arylation of amines via Ullmann-type coupling reactions, facilitating the formation of C–N bonds between aryl halides and amines. The catalyst proved to be highly stable, maintaining its catalytic performance for at least seven consecutive cycles without significant degradation. Ding et al. reported a non-toxic and cost-effective Fe complex (iron ethylene-1,2-diamine) over carbon nanotubes (CNTs) as a single-atom heterogeneous catalyst (Fe-Nx/CNTs) for C–N bond formation reaction from aromatic amines and ketones [97]. The synthesized catalyst exhibited high efficacy in this process, demonstrating a wide range of substrate variety. Furthermore, the catalyst also demonstrated industrial potential by being reusable for seven cycles without significant activity loss.



Scheme 6. Representation of some significant Buchwald–Hartwig amination products synthesized using recently reported heterogeneous Fe catalysts [88,90,92].

In another work, Sun et al. demonstrated a fascinating protocol for the synthesis of single-atom Fe catalyst ($\text{Fe}_1\text{-N-C}$) derived from zeolitic imidazolate frameworks (ZIF), for selective ammoxidation reactions, i.e., the elimination reaction between a benzyl alcohol and aqueous NH_3 [98]. The reported $\text{Fe}_1\text{-N-C}$ catalyst was proven to be very efficient for the synthesis of various nitriles ($-\text{CN}$) from alcohols in water under mild conditions, offering chemo selectivity, recyclability, and high efficiency. Most importantly, this $\text{Fe}_1\text{-N-C}$ catalyst was a valuable addition for nitrile synthesis, important in fine chemical industry as well as other research sectors. Another effective method for forming single C–N bonds from stable and easily accessible substrates, such as amines and alcohols, is hydrogen auto transfer amination, often known as borrowing hydrogen [99]. Many believe it to be the most environmentally friendly and atom-efficient way to make complex amines [100].

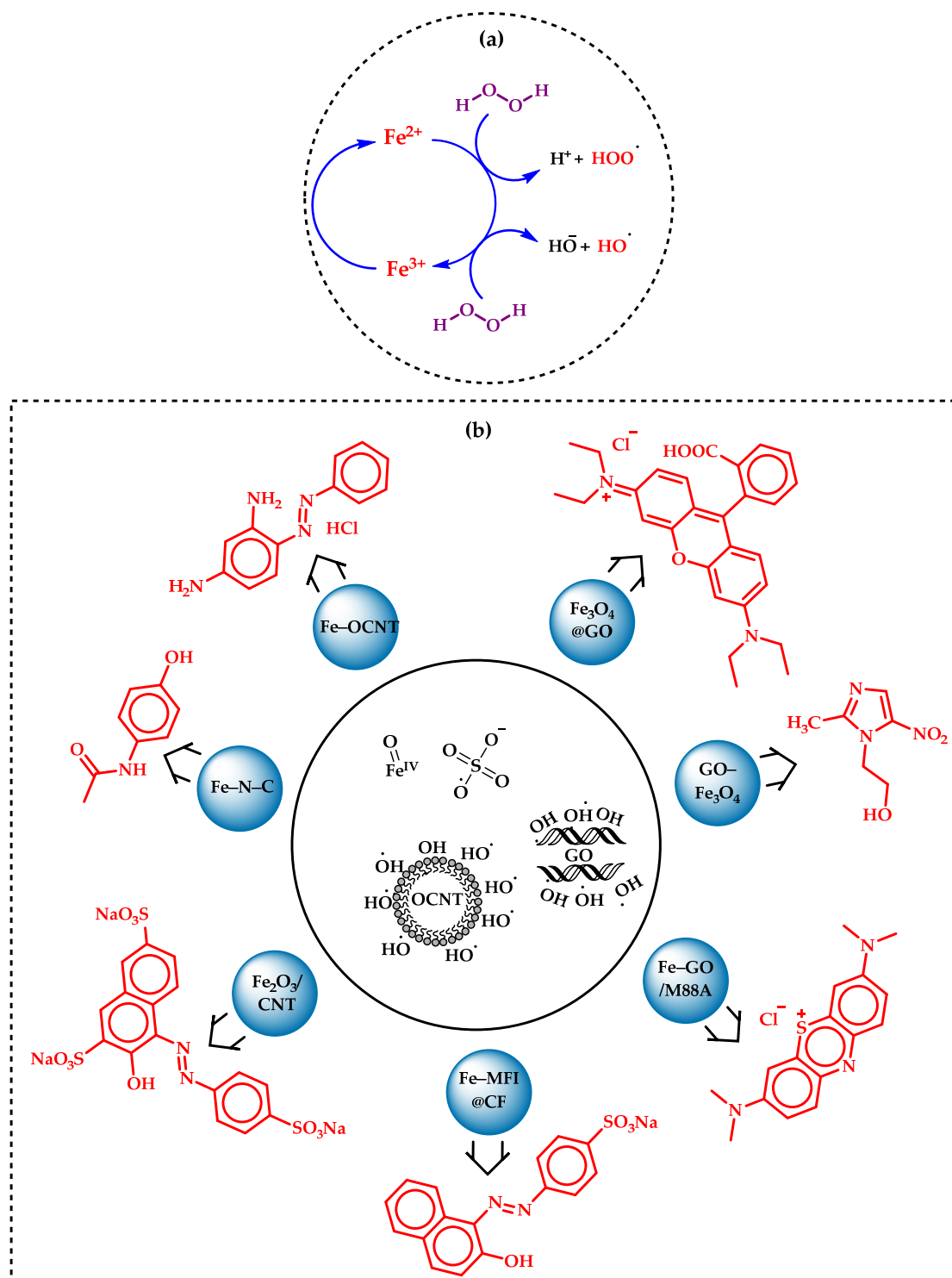
5. Oxidation Reactions

Organic oxidation reactions are considered to be one of the well-studied and significant organic transformation reactions due to their versatile applicability in different sectors like fine chemicals, pharmaceuticals, drug, and dye synthesis [101,102]. These reactions are significant in both industrial and environmental contexts due to their efficiency and sustainability [102]. Typically, Fe catalysts can activate oxidants like hydrogen peroxide (H_2O_2), molecular oxygen (O_2), or organic peroxides to oxidize substrates, including hydrocarbons, alcohols, olefins, and heterocycles [101]. The reactions often proceed under mild conditions, showcasing the high selectivity and yield of the desired product [102]. Advances in this field continue to optimize catalytic performance, enhancing reaction rates, and minimizing by-products.

5.1. Advanced Oxidation Process by Fenton's Reaction

The first thing one needs to counteract an Fe-catalyzed oxidation reaction is the advanced oxidation process (AOP) or Fenton's process for the degradation of organic pollutants in waste water remediation [103]. Unlike the traditional Fenton reaction, which uses soluble Fe salts, the heterogeneous variant employs solid Fe catalysts, such as Fe oxides or Fe-impregnated materials [104]. In this process, the solid iron catalyst activates H_2O_2 to generate hydroxyl radicals ($\bullet\text{OH}$), which are highly reactive and can effectively break down a wide range of organic contaminants [105]. The key advantages of the heterogeneous Fe-catalyzed Fenton reaction include easier recovery and reuse of the catalyst, reduced Fe sludge production, and enhanced stability under various environmental conditions [105]. This method is particularly effective in treating wastewater containing persistent organic pollutants, dyes, and pharmaceuticals [105]. Recent developments in this field focus on improving the catalytic activity, stability, and surface properties of the Fe-based materials [105]. Researchers are also exploring various supports, such as activated carbon, silica, and clays, to enhance the dispersion and accessibility of the Fe active sites [106]. These advancements aim to increase the efficiency and cost-effectiveness of the heterogeneous Fenton reaction, making it a promising solution for large-scale environmental remediation efforts [106]. Recently, Peng et al. created a single Fe-atom N-doped carbon matrix (Fe-N-C) as a superior heterogeneous catalyst for the activation of peroxydisulphate (PDS) to degrade dissolved pollutants like paracetamol, ciprofloxacin, Bisphenol-A, etc., from waste water [107]. Interestingly, the N-doped carbon cluster was derived from pyrolysis of a sea water pollutant, namely 'Enteromorpha' at 900 °C. Radical quenching and electrochemical investigation confirm high-valence Fe-oxo species and an electron-transfer pathway for nonradical oxidation. Another study explaining the activation of PDS was also reported by Madihi-Bidgoli et al., in which a carbon nanotube (CNT)-encapsulated Fe_2O_3 nanocatalyst was used for photocatalytic azurobine degradation under UVA-LED irradiation [108]. The azurobine degradation was found to be more accelerated by sulphate radicals than $\bullet\text{OH}$ radicals. The recyclability of the material was also analyzed and the response was found to be positive with a good number of catalytic cycles. Chen et al. designed a CNT-supported heterogeneous Fenton-like system, Fe-OCNT, for selective oxidation of methylene blue

(MB) and chrysoidine G [109]. The catalyst, Fe-OCNT, fabricated by attaching Fe ions to the surface of oxidized CNT, was allowed to activate H_2O_2 , and then the Fenton's process was followed. This selective oxidation is attributed to $\bullet OH$ radicals adsorbed on the CNT surface. This selective oxidation system is found to be effective across a broad pH range (4.0 to 9.0), with excellent resistance to traditional $\bullet OH$ radical quenching agents.



Scheme 7. (a) Classical pathway of Fenton's process, (b) AOP performed by some reported heterogeneous Fe catalysts (blue) along with the degradative pollutants (red). The inset circle represents the active species of AOP.

Xie et al. demonstrated a graphene oxide (GO)-supported heterogeneous Fe-MOF (Fe-GO/M88A) for a photocatalytic Fenton reaction aimed at water purification [110]. This MOF exhibited significantly improved the catalytic efficiency of MB separation from water samples. The GO/M88A catalyst was effectively treated with urban textile wastewaters and demonstrated high degradation efficiency for MB (98.81%) and bisphenol-A (97.27%) as a catalyst in a photo-Fenton degradation process. These findings highlight the potentiality of the GO/M88A membrane for water purification and environmental protection applications due to its excellent separation performance, stability, and photo-Fenton activity. Dye-polluted wastewater was treated via AOP by Pervez et al. using Fe₃O₄-impregnated GO system (Fe₃O₄@GO) followed by activation with persulfate (K₂S₂O₈) [111]. This method efficiently degraded Rhodamine B (RhB) to 95% from 25% with Fe₃O₄ alone. Nevertheless, after repeated usage, the system retained its true catalytic activity as well as low Fe leaching. Considering the degradation mechanism, rather than the •OH radicals the surface-bound SO⁴⁻ was found to be the active species for RhB breakdown. Görmez et al. demonstrated an electro-Fenton process using a GO immobilized Fe₃O₄ catalyst for the mineralization and breakdown of chloramphenicol and metronidazole antibiotics [112]. The mineralization rate for chloramphenicol was reported to be 73% and that for metronidazole was 86%. Remarkably, over ninety-nine percent of these antibiotics were found to be degraded using this GO-Fe₃O₄ catalyst. Afterwards, the durability of the catalyst in these hazardous conditions was shown by its capacity to maintain its heterogeneity for minimum of four consecutive electro-Fenton cycles. Again, Le et al. synthesized an Fe-rich MFI-zeolite-modified carbon felt (CF) material, Fe-MFI@CF, as a heterogeneous catalyst in an electro-Fenton (EF) process for the degradation of acid orange 7 (AO7) [113]. The MFI@CF catalyst was reported to catalyze the full degradation of AO7 (0.1 mM) in 40 min. However, the system exhibited encouraging efficacy, achieving a 26.6% reduction in total organic carbon (TOC) after 8 h at a pH level of 6.5. Scheme 7 depicts some significant Fe-based heterostructures for AOP in waste water remediation.

5.2. Oxidation of Benzyl Alcohols

Selective oxidation of benzyl alcohols (BAs) to benzaldehydes (BALs) is a crucial transformation in organic chemistry, often used to synthesize fine chemicals and pharmaceuticals [114]. Benzaldehyde is a highly significant and versatile organic compound that has extensive utility in various industrial applications [115]. This process typically involves using various catalysts, including metal-based, metal-free, and heterogeneous catalysts, to achieve high selectivity and efficiency [116–118]. Fe-catalyzed selective oxidation of BAs to BALs is an efficient and environmentally friendly process [119]. Fe-based catalysts facilitate the oxidation reaction under mild conditions, often using O₂ or H₂O₂ as the oxidant. This method provides a high selectivity for BAL with minimal over-oxidation to benzoic acid. The process is notable for its use of readily available and non-toxic Fe catalysts, making it a sustainable choice for industrial applications. Additionally, these catalysts can often be reused without significant loss of activity, enhancing the overall efficiency and cost-effectiveness of the oxidation process. Lots of reports are available in literature for the Fe-catalyzed selective oxidation of BAs to BALs. Crombie et al. synthesized a heterogeneous catalyst of Pd-Fe alloys supported on titania (TiO₂) as an efficient catalyst in the specific oxidation of BA to BAL without any external oxidizing agent [118]. This mechanism of the studied reaction depends on the in situ generation of H₂O₂ from molecular hydrogen (H₂) and O₂, and interestingly, the reaction did not take place with molecular O₂ alone. The oxidation rate of BA was found to be much greater when utilizing supported Pd-Fe NPs as compared to Pd-Au or Pd-only counterparts. A mild method for fabricating spherical NiFe₂O₄ NPs as a catalyst for selectively oxidizing BA to BAL was presented by Iraqui et al. [120]. This nanocatalyst displayed a high oxidation ability with 85% conversion of BA and 100% selectivity using tert-butyl hydroperoxide (TBHP) at 60 °C in 3 h. Owing to its magnetic behavior, the NiFe₂O₄ nanocatalyst was easily separable and reusable for up to five consecutive cycles without hampering catalytic activity.


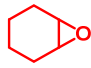
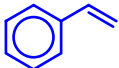
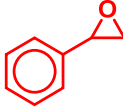
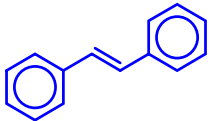
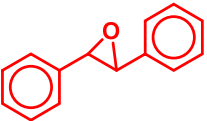
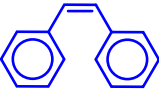
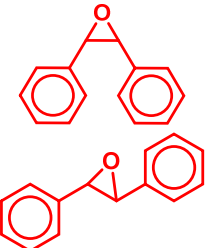

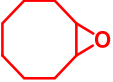
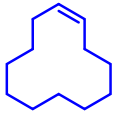
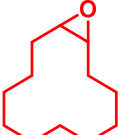
The comparative rates of oxidation of BAs to BALs in O₂ and H₂O₂ environments were investigated by Baruah et al. over an Fe₂O₃ photocatalyst embedded in halloysite nanotubes (HNTs) [121]. The catalysis results demonstrated that the Fe₂O₃-HNT nanocatalyst achieved greater activity in the presence of the H₂O₂ oxidant than O₂. The mechanism of oxidation was also investigated by electron spin resonance (ESR) and Raman spectroscopic analysis, which provided direct evidence of the involvement of superoxide radical bound Fe (III) species in the BA oxidation reaction. Owing to its suitable band gap (~2.14 eV), the catalyst enabled absorption under visible light irradiation. A new synthesis method was represented by Wei et al. for the preparation of a Mott–Schottky type N-doped carbon-supported single-atom Fe (SA-Fe/Nx-C) catalyst for the selective oxidation of BA to BAL with superior catalytic ability [122]. The N source of the catalyst was appeared from carbon nitride which also acted as a templating agent during the catalyst synthesis. The high catalytic activity was attributed to the tetra-coordinated FeN₄ structure of the material, which facilitates electron transfer from metallic Fe to N atoms at the Mott–Schottky interface. Furthermore, the systematic introduction of N into carbon through the precise manipulation of the carbon nitride ratio during catalyst synthesis facilitated the modulation of electron transfer in metallic Fe. Consequently, this approach significantly improved the selectivity of BA oxidation. In the meantime, the core–shell nanocatalysts gained significant importance in the catalysis sector due to their unique properties and diverse applications in different areas [123,124]. These structures consist of a core material surrounded by a shell of another material, offering synergistic effects and enhanced functionalities compared to their individual components [123,125]. Recently, Xu et al. introduced Fe₃O₄-based core–shell nanocatalysts (Fe₃O₄@Cu₂O) and Fe₃O₄@Cu₂O–Cu for the aerobic oxidation of BAs to BALs, employing 2,2,6,6-tetramethylpiperidine-N-oxyl (TEMPO) and N-methylimidazole (NMI) as co-catalysts [126]. When combined with both TEMPO and NMI, these materials exhibited excellent catalytic activities in the aerobic oxidation of BAs under ambient conditions. The materials demonstrated recyclability and robustness, maintaining activity with less than a 10% drop in performance over seven consecutive runs. Their magnetic properties of these materials facilitated the easy separation after the reaction using an external magnet. The facile synthesis and catalytic performance of a newly synthesized core–shell α-Fe₂O₃@Au nanocomposite were emphasized by Paul et al. [127]. The reported results evident for the excellent catalytic performance of the α-Fe₂O₃@Au in BA oxidation, with up to five repeated catalytic cycles. Moreover, Zheng et al. derived a magnetically retrievable core–shell photocatalyst of Fe₃O₄, cadmium sulfide (CdS), and carbon quantum dots (CQDs), Fe₃O₄@CdS@CQDs, for the selective oxidation of BA with in situ generated H₂O₂ [128]. Additionally, novel Z-scheme photocatalysis was found to follow the mechanistic route of the oxidation process. The outcomes of BA oxidation by recently reported Fe heterostructures are summarized in Table 1.

Table 1. Significant Fe-based heterostructures recently reported for BA oxidation reaction.

| Entry | Catalyst | Oxidant | % Conv. (BA) | % Sel. (BAL) | % Yield (BAL) | Ref. |
|-------|---|--|--------------|--------------|---------------|-------|
| 1 | Pd-Fe@TiO ₂ | H ₂ O ₂ | 97 | 100 | — | [118] |
| 2 | NiFe ₂ O ₄ NPs | TBHP | 85 | 100 | — | [120] |
| 3 | Fe ₂ O ₃ -HNT | O ₂ , H ₂ O ₂ | 88, 92 | 100, 100 | — | [121] |
| 4 | SA-Fe/Nx-C | O ₂ | 92 | 97 | — | [122] |
| 5 | Fe ₃ O ₄ @Cu ₂ O | air | — | 99 | 99 | [126] |
| 6 | α-Fe ₂ O ₃ @Au | air | — | 98 | 96 | [127] |

% Conv. (% conversion), % Sel. (% selectivity), and the reaction conditions are as per the respective article.

Table 2. Olefin epoxidation results of reported Fe-N/C and Fe/PMA@CIN-1 catalysts [129,130].

| Catalyst | Oxidant | Reactant | Product(s) | % Conv. ^[a] | % Yield | % Sel. ^[b] |
|--------------|---|---|---|------------------------|---------|-----------------------|
| Fe-N/C | O ₂ (1 atm) |  |  | 99 | 91 | 91 |
| | |  |  | 70 | 17 | 12 |
| | |  |  | 78 | 67 | 52 |
| | |  |  | 79 | 96 | 76 |
| Fe/PMA@CIN-1 | H ₂ O ₂ (1 mmol) |  |  | 88 | — | 99 |
| | |  |  | 58 | — | 99 |

Solvent: acetonitrile (CH₃CN), Time: 6–17 h (Fe-N/C) and 8 h (Fe/PMA@CIN-1), Temperature: Room temperature (Fe-N/C) and 80 °C (Fe/PMA@CIN-1), % Conv. ^[a] = % conversion of the olefin, % Sel. ^[b] = % selectivity of the epoxide.

5.3. Epoxidation Reactions

The epoxidation reaction offers a sustainable and efficient method for synthesizing epoxides, important intermediates in organic synthesis [131]. Epoxides are highly valuable intermediates and building blocks in the synthesis of various chemicals, including pharmaceuticals, agrochemicals, and fine chemicals [132]. Epoxidation can be achieved through different methods, such as using peracids, peroxyacids, or metal-catalyzed processes [133]. Among these, metal-catalyzed epoxidation reactions, particularly those involving transition metals like Ti, Co, Cu, and Fe, have gained significant attention due to their efficiency, selectivity, and compatibility with diverse functional groups [134–136]. These reactions play a crucial role in the synthesis of complex molecules and are essential tools in the repertoire of synthetic chemists [136]. Malko et al. synthesized a heterogeneous Fe-incorporated carbon-supported catalyst for effective epoxidation of cyclic olefins (like cyclohexene) in O₂ environment [129]. This recyclable catalyst was reported to successfully produce the desired epoxidation products with a very high % yield (Table 2). Yu et al. developed an Fe and phosphomolybdic acid (PMA) immobilized covalent organic framework (COF), Fe/PMA@COF, for the selective and efficient epoxidation of cyclooctene with H₂O₂ (Table 2) [130]. This report on the Fe-immobilized COF presented an extraordinary heterogeneous catalyst that efficiently oxidized olefins in an inexpensive way, and displayed the magnificent properties of the COF as the catalytic support for such reactions. In the field of chemical industry, another significant epoxidation reaction is transition-metal-catalyzed styrene epoxidation, because the resulting product, styrene oxide, serves as a

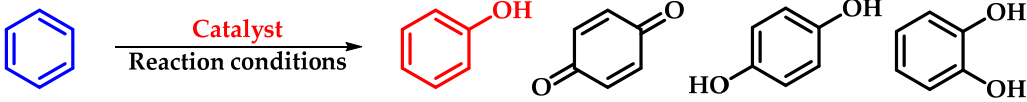
key building block for the production of various invaluable chemicals, including plastics, pharmaceuticals, and fine chemicals [137,138]. Epoxidized styrene derivatives also find applications in polymerization reactions to produce polystyrene and as intermediates in the synthesis of surfactants, detergents, and epoxy resins [139,140]. Recently, Yang et al. synthesized an amorphous alumina (Al_2O_3)-supported FeO_x heterogeneous catalyst for the selective conversion of styrene-to-styrene oxide with a high catalytic efficiency [137]. Fe atoms were regarded to enhance the adsorption of styrene onto the catalytic active sites of the clusters, paving the way for epoxidation. Additionally, the defective structure of the amorphous Al_2O_3 nanosheet also triggered the reactivity of the catalyst by preventing the FeO_x moieties from agglomeration during the epoxidation process. Recently, a magnetic Fe_3O_4 core and a porous CuSiO_3 combined heterogeneous core-shell nanocatalyst was designed by Wu et al. for a highly selective styrene epoxidation reaction [141]. The catalyst outperformed pure Fe_3O_4 , pure CuSiO_3 , or a physical combination of the two in styrene epoxidation with TBHP. Because of its great stability and ease of recycling, it maintained its catalytic activity and structural integrity even after six uses. Similarly, Liu et al. developed a heterogeneous spinal cobalt ferrate nanocatalyst, CoFe_2O_4 , for styrene epoxidation with TBHP as the oxidant [142]. The activity of this spinal on epoxide generation was reported to significantly outperform its monometallic equivalents i.e., Co_3O_4 flakes and Fe_2O_3 rods. Due to its large surface area, mesoporous structure, and abundance of surface metal redox couples resulting from its bimetallic structure, the CoFe_2O_4 produced a remarkable catalytic activity. However, the material retained its true catalytic ability as well as heterogeneity for up to five consecutive runs.

5.4. Hydroxylation Reactions

Hydroxylation reactions are crucial in both biological and synthetic chemistry, playing a key role in the metabolism of various substances and the synthesis of complex molecules [143,144]. In biological systems, hydroxylation is often mediated by enzymes such as cytochrome P450 monooxygenases, which facilitate the oxidation of organic substrates [145]. In industrial and laboratory settings, hydroxylation can be achieved using a variety of catalysts and oxidizing agents, enabling the production of valuable chemicals, pharmaceuticals, and intermediates for further chemical transformations [146–149]. Considering Fe-catalyzed hydroxylation reactions, Salazar-Aguilar et al. derived an Fe-based MOF, Fe-BTC for the direct hydroxylation of phenol to synthesize dihydroxy benzene in the presence of H_2O_2 [150]. The active species of the hydroxylation to occur was reported as $\bullet\text{OH}$ species from H_2O_2 breakdown. Very recently, a recyclable nanocatalyst for benzene hydroxylation was created by Wu et al. using cupric acetylacetonate grafted Fe-doped mesoporous silica (Cu/Fe-SBA-15) with extensively scattered metallic sites [151]. Owing to the synergistic effect of the doped Fe sites and the grafted Cu sites, the synthesized Cu/Fe-SBA-15 catalyst showed outstanding catalytic activity in the direct hydroxylation of benzene with H_2O_2 as the oxidant. Yue et al. also designed an MFI-zeolite-supported Fe-based catalyst (Fe-MFI zeolite) for the H_2O_2 mediated hydroxylation of benzene [152]. Compared to the pure silica zeolite seed sol, Fe-MFI zeolite exhibits a higher conversion of 12.1% of benzene with a selectivity of 97% at 60 °C during the reaction in H_2O_2 environment. Focusing on the effects of the ion-exchange sequence on the physicochemical and catalytic characteristics, Xiao et al. investigated an Fe, Cu-based bimetallic catalyst over zeolite support, Fe-Cu/beta zeolite [153]. When subjected to benzene hydroxylation with H_2O_2 , the catalyst displayed outstanding catalytic activity with a ~43% conversion of benzene with ~96% product selectivity. Another efficient Fe-based catalyst for benzene hydroxylation was reported by Lu et al. through covering Fe NPs with a layer of N-doped carbon (Fe@NC) [154]. The carbon shells prevented Fe leaching and enhance selective benzene adsorption with their hydrophobic surface. However, Fe@NC displayed very good selectivity and long-lasting catalytic efficacy of benzene hydroxylation with 16% yield of phenol and 95% selectivity. Similarly, another core-shell carbon encapsulated Co-Fe nanostructure was designed by Zeng et al. for the highly selective hydroxylation of

phenolic compounds [155]. The catalyst achieved higher results, with 27% phenol with 97% selectivity. The selective hydroxylation of benzene to phenol by some interesting Fe-based catalysts is depicted in Table 3.

Table 3. Selective hydroxylation of benzene to phenol by some reported Fe-based heterostructures [149,151–154].



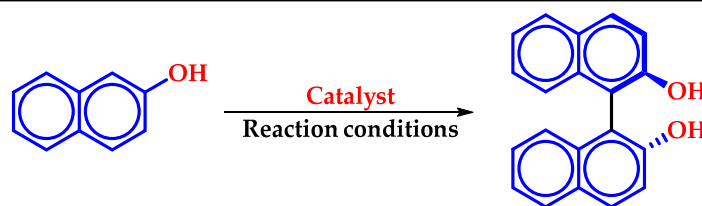
The reaction scheme shows benzene (a blue hexagon) reacting with a catalyst under reaction conditions to produce phenol (a red hexagon with an OH group), 1,4-benzoquinone (a six-membered ring with two double bonds and two carbonyl groups), 1,4-dihydroxybenzene (a benzene ring with two OH groups at the para position), and 1,2-dihydroxybenzene (a benzene ring with two OH groups at the ortho position).

| Entry | Catalyst | Amount (mg) | Temp. (°C) | Time (h) | % Sel. (Phe.) |
|-------|--|-------------|------------|----------|---------------|
| 1 | Fe-MFI-Zeolite | 100 | 60 | 2 | 97 |
| 2 | Fe-Cu/Beta Zeolite | 50 | 60 | 6 | 96 |
| 3 | Cu-Fe/SBA-15 | 30 | 60 | 3 | 93 |
| 4 | Fe-NC | 30 | 60 | 4 | 95 |
| 5 | CuO-Fe ₂ O ₃ /Fe ₃ O ₄ | 50 | 40 | 24 | 85 |

All the reactions were performed in CH₃CN solvent and H₂O₂ as oxidant, Temp. = Temperature, % Sel. (Phe.) means % Selectivity of phenol.

5.5. Oxidative Coupling Reactions

An oxidative coupling reaction is a chemical process in which two molecules or molecular fragments are joined together with the concurrent oxidation of a substrate [156,157]. The process can be catalyzed by various metals, including iron, copper, and palladium, which facilitate the removal of electrons from the substrates, promoting their coupling [158]. Oxidative coupling is widely used in organic synthesis to construct complex molecular structures efficiently and selectively [158]. One of the oxidative coupling reactions that has received a lot of attention is the selective production of BINOL from 2-naphthol [159]. According to the literature, this coupling reaction may be facilitated by a variety of metal catalysts, including salts, metal Schiff-base complexes, metal NPs supported on inorganic mantles, and metal oxide nano catalysts [160,161]. Out of the various transition metal catalysts, Fe-based catalysts are known to be most effective for such conversion [162,163]. The majority of the studies focus on using O₂ as an oxidant, whereas there are only a countable number of articles that address the selective oxidation of 2-naphthol when H₂O₂ is present. When 2-naphthol is oxidized with H₂O₂, it produces 1,2-dihydroxynaphthalene and 1,2-naphthoquinone as by-products; however, the yield of BINOL is very low. In the presence of O₂, the observed reaction time is considerably longer because O₂ is a mild oxidant. Although the oxidant H₂O₂ (30% *w/v*) is effective in converting a significant portion of the reactant quickly, it often lacks control over selectivity during the reaction. Interestingly, Baruah et al. also apply the HNT-embedded Fe(III) catalyst (Fe₂O₃-HNT) for the oxidative coupling of 2-naphthol to synthesized selective BINOL [121]. On the other hand, enantioselective oxidation of 2-naphthol has gained a lot of interest due to the versatilities of chiral (R/S) BINOL derivatives in different areas. Interestingly, Horibe et al. developed chiral Fe(II)-di-phosphine oxide complexes for the selective synthesis of chiral BINOL via oxidative coupling reactions [163]. This chiral catalyst exhibited excellent activity of R-BINOL production up to 98% yield with 68% enantiomeric excess (ee). Similarly, Wu et al. also demonstrated an efficient protocol of the synthesis of chiral BINOL through an in situ generated Fe catalyst by enantioselective oxidative coupling of 2-naphthol [162]. The catalyst was synthesized by simultaneous addition of Iron(II) perchlorate hydrate and a bis-quinolyl diamine ligand [(1*R*,2*R*)-*N*¹,*N*²-di(quinolin-8-yl) cyclohexane-1,2-diamine along with the 2-naphthol reaction mixture. Different 2-naphthol derivatives were also analyzed by this method and it was noted that moderate to good outcomes were attained with the formation of respective R-BINOL derivatives in terms of % yield and ee. However, to the best of our knowledge, Fe-based heterogeneous chiral catalysts have not been widely used for such enantioselective oxidation reactions. Table 4 represents some recently reported Fe-based catalysts for the oxidative coupling of 2-naphthol to BINOL.

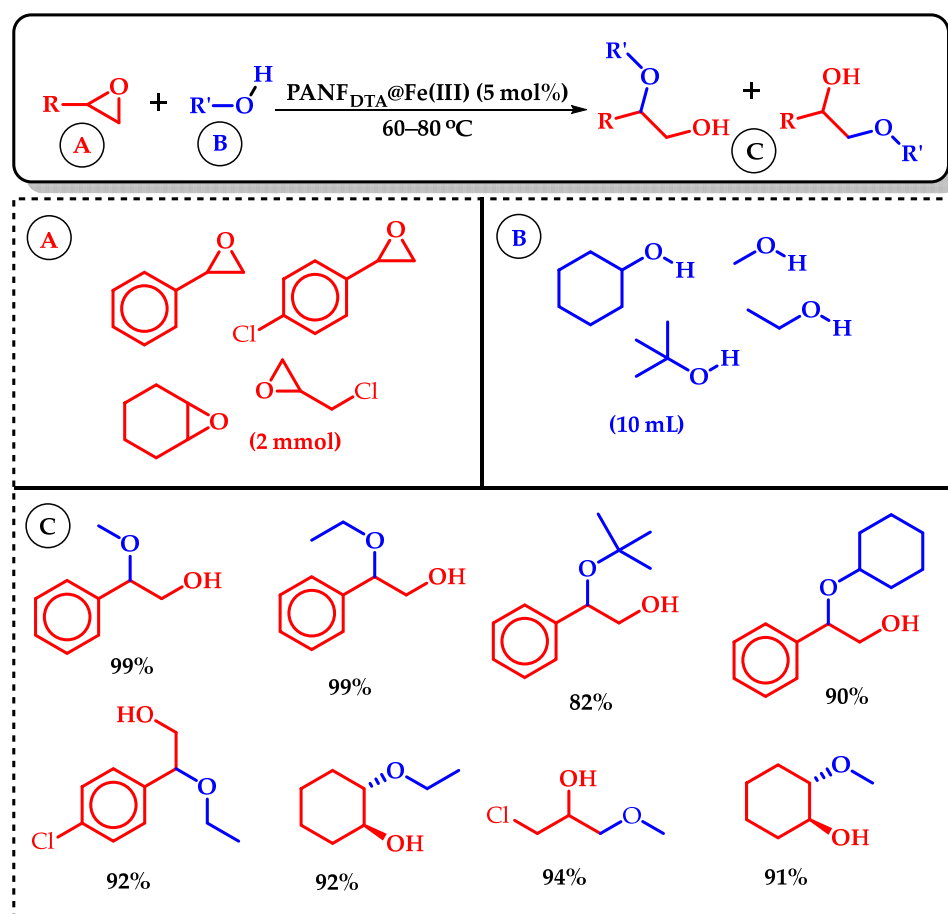
Table 4. Results of oxidative coupling of 2-naphthol to BINOL by some recently reported Fe catalysts.

| Entry | Catalyst | Amount | Oxidant | Temp. | Time (h) | % Yield ^[a] | % ee ^[b] | Subs. ^[c] |
|-------|-------------------------------------|---------|--|-----------|----------|------------------------|---------------------|----------------------|
| 1 | Fe ₂ O ₃ -HNT | 30 mg | O ₂ , H ₂ O ₂ | RT | 2, 1 | 89, 72 | – | 1 |
| 2 | Fe(OTf) ₂ -ligand | 5 mol% | TBHP | –20–10 °C | 60 | 77–98 | 6–70 | 19 |
| 3 | Fe(ClO) ₄ -ligand | 10 mol% | O ₂ | 50 °C | 5–18 | 51–99 | 12–62 | 12 |
| 4 | [Fe(salen)-ν-(OH)] ₂ | 4 mM | O ₂ | 60 °C | 72 | 87 | – | 1 |

The reactions were performed in CH₃CN solvent, except for [Fe(salen)-n-(OH)]₂ which was performed in toluene, RT = Room Temperature, % Yield ^[a] = % Yield of BINOL, % ee ^[b] = % enantiomeric excess of R-BINOL, Subs. ^[c] = substrate diversity.

6. Epoxide Ring Opening Reactions

Epoxide ring opening is a fundamental organic reaction catalyzed by acids, bases, or nucleophiles, wherein an epoxide molecule undergoes cleavage to form a diol or other functionalized products [164–166]. Mechanistically, the reaction involves the attack of a nucleophile at the electrophilic carbon of the epoxide ring, leading to the formation of a new bond and opening of the ring [167,168]. Epoxide ring opening reactions are widely employed in organic synthesis to construct complex molecules and functionalize organic compounds with diverse applications in pharmaceuticals, materials science, and fine chemicals [169–171]. Typically, transition metals such as Ti, Al, Zn, and Fe serve as catalysts [169–173]. Nagarjun et al. synthesized an Fe-based MOF, MIL-101(Fe), as a highly active, regioselective heterogeneous Lewis-acid catalyst for ring-opening styrene oxide [174]. The MIL-101(Fe) exhibited superior catalytic activity of styrene epoxide ring opening by indole and its derivatives as a nucleophile with a 70–90% yield of the desired product. Furthermore, the heterogeneity of the catalyst was confirmed through leaching tests, and its activity was maintained over four catalytic cycles. Shi et al. derived a polyacrylonitrile fiber (PAN F_{DTA}) supported Fe(III) heterogeneous catalyst for epoxide ring opening reaction [175]. In presence of the catalyst, the reaction proceeded with methanol as the nucleophile and demonstrated ~80–99% yield of the open-chain β-methoxy alcohol product (Scheme 8). In addition, the catalyst maintained its properties during long-term storage without additional protection, and there was no discernible decline in the catalytic activity for recycling over 20 cycles. Wang et al. synthesized molecular sieve (PKU-1) supported Fe catalyst, Fe-PKU-1 for ring opening of cyclohexanone using water as the nucleophilic agent [176]. It was reported that both the S_N¹ and S_N² pathways are favored by the reaction for the selective production of *trans*-1,2-cyclohexanediol over the *cis*-form with excellent yield. Moreover, the Fe-PKU-1 is reported to be stable for up to five catalytic cycles without hampering the % yield as well as the selectivity of the *trans*-diol.



Scheme 8. Ring opening of epoxides catalyzed by PANF_{DTA}@Fe(III) reported by Shi et al. [175]. In the scheme, A and B are the reactants, and C is the product. The % yields of Cs are mentioned with the respective structure.

7. Future Perspectives

In the realm of organic synthesis, the future of heterogeneous Fe catalysis holds promising prospects. With ongoing advancements in catalytic methodologies, Fe-based catalysts are poised to play a pivotal role in sustainable and environmentally friendly organic transformations. Leveraging the abundance, low cost, and eco-friendliness of iron, researchers are exploring innovative approaches to enhance the efficiency, selectivity, and scope of Fe-catalyzed reactions. Moving forward, one can anticipate the development of novel Fe-based catalysts with tailored structures and compositions, aimed at addressing specific challenges in organic synthesis. This includes the design of heterogeneous catalysts with well-defined active sites, improved stability, and enhanced catalytic performance under mild reaction conditions. Moreover, the integration of Fe catalysis with emerging technologies, such as flow chemistry and photochemistry, offers exciting avenues for efficient and selective organic transformations. Harnessing the synergistic effects of Fe catalysis with these advanced techniques can enable the development of streamlined processes with reduced energy consumption and waste generation. Furthermore, exploring the catalytic potential of Fe-based materials in tandem with sustainable reaction media and renewable feedstocks holds promise for greener and more sustainable chemical synthesis. The integration of Fe catalysis with biocatalysis and cascade reactions could lead to the development of efficient and environmentally benign synthetic routes for the production of valuable organic molecules. Briefly, the future of heterogeneous Fe catalysis in organic synthesis is characterized by innovation, sustainability, and versatility. By harnessing the unique properties of iron and leveraging advancements in catalytic design and methodologies,

Fe-based catalysts are poised to make significant contributions to the development of efficient and sustainable synthetic routes for diverse organic transformations.

8. Conclusions

The application of heterogeneous Fe catalysis in these diverse transformations underscores its versatility and potential as a sustainable and cost-effective alternative to precious metal catalysts. By harnessing the unique reactivity of Fe, chemists have been able to develop innovative synthetic methodologies that are not only efficient and selective but also environmentally benign. Moreover, the abundance and low cost of Fe make these catalysts accessible to a wide range of researchers, both in academia and industry, facilitating the further exploration and development of heterogeneous Fe-based catalytic systems.

Author Contributions: M.J.B.: Conceptualization, validation, formal analysis, resources, writing—original draft preparation, review and editing, visualization; R.D.: software, resources, validation; M.E.A.Z.: Validation, formal analysis, investigation, resources, writing—original draft preparation, review and editing, supervision; K.K.B.: Conceptualization, validation, formal analysis, investigation, resources, writing—original draft preparation, review and editing, supervision, funding acquisition. All authors have read and agreed to the published version of the manuscript.

Funding: This research was funded by Council of Scientific and Industrial Research (CSIR), India Grant No. 80(0094)/20/EMR-II, Science and Engineering Research Board (SERB), Department of Science and Technology, Government of India grant No. CRG/2023/000957 and EEQ/2023/000350.

Institutional Review Board Statement: Not applicable.

Informed Consent Statement: Not applicable.

Data Availability Statement: No new data were created or analyzed in this study.

Conflicts of Interest: The authors declare no conflict of interest.

References

1. Tietze, L.F. Domino Reactions in Organic Synthesis. *Chem. Rev.* **1996**, *96*, 115–136. [[CrossRef](#)] [[PubMed](#)]
2. Norbert, H. Photochemical Reactions as Key Steps in Organic Synthesis. *Chem. Rev.* **2008**, *108*, 1052–1103.
3. Xiao, J.; Liu, X.; Pan, L.; Shi, C.; Zhang, X.; Zou, J.J. Heterogeneous Photocatalytic Organic Transformation Reactions Using Conjugated Polymers-Based Materials. *ACS Catal.* **2020**, *10*, 12256–12283. [[CrossRef](#)]
4. Vekariya, R.L. A Review of Ionic Liquids: Applications Towards Catalytic Organic Transformations. *J. Mol. Liq.* **2017**, *227*, 44–60. [[CrossRef](#)]
5. Chng, L.L.; Erathodiyil, N.; Ying, J.Y. Nanostructured Catalysts for Organic Transformations. *Acc. Chem. Res.* **2013**, *46*, 1825–1837. [[CrossRef](#)]
6. Li, Z.; Brouwer, C.; He, C. Gold-Catalyzed Organic Transformations. *Chem. Rev.* **2008**, *108*, 3239–3265. [[CrossRef](#)]
7. Cheng, W.M.; Shang, R. Transition Metal-Catalyzed Organic Reactions Under Visible Light: Recent Developments and Future Perspectives. *ACS Catal.* **2020**, *10*, 9170–9196. [[CrossRef](#)]
8. Lyons, T.W.; Sanford, M.S. Palladium-Catalyzed Ligand-Directed C–H Functionalization Reactions. *Chem. Rev.* **2010**, *110*, 1147–1169. [[CrossRef](#)]
9. Labinger, J.A. Platinum-Catalyzed C–H Functionalization. *Chem. Rev.* **2017**, *117*, 8483–8496. [[CrossRef](#)]
10. Naota, T.; Takaya, H.; Murahashi, S.I. Ruthenium-Catalyzed Reactions for Organic Synthesis. *Chem. Rev.* **1998**, *98*, 2599–2660. [[CrossRef](#)]
11. Rana, S.; Biswas, J.P.; Paul, S.; Paik, A.; Maiti, D. Organic Synthesis with the Most Abundant Transition Metal–Iron: From Rust to Multitasking Catalysts. *Chem. Soc. Rev.* **2021**, *50*, 243–472. [[PubMed](#)]
12. Bauer, I.; Knolker, H.J. Iron Catalysis in Organic Synthesis. *Chem. Rev.* **2015**, *115*, 3170–3387. [[PubMed](#)]
13. Zhu, F.; Lu, G.P.; Wang, F.; Ren, E.; Yu, Y.; Lin, Y. Iron Catalyzed Organic Reactions in Water: A “Nature-Like” Synthesis. *Curr. Opin. Green Sustain. Chem.* **2023**, *40*, 100754. [[CrossRef](#)]
14. Pellissier, H. Recent Developments in Enantioselective Iron-Catalyzed Transformations. *Coord. Chem. Rev.* **2019**, *386*, 1–31. [[CrossRef](#)]
15. Sun, C.L.; Li, B.J.; Shi, Z.J. Direct C–H Transformation via Iron Catalysis. *Chem. Rev.* **2011**, *111*, 1293–1314. [[CrossRef](#)]
16. Chughtai, A.H.; Ahmad, N.; Younus, H.A.; Laypkov, A.; Verpoort, F. Metal–Organic Frameworks: Versatile Heterogeneous Catalysts for Efficient Catalytic Organic Transformations. *Chem. Soc. Rev.* **2015**, *44*, 6804–6849. [[CrossRef](#)]
17. Kumar, P.; Tomar, V.; Kumar, D.; Joshi, R.K.; Nemiwal, M. Magnetically Active Iron Oxide Nanoparticles for Catalysis of Organic Transformations: A Review. *Tetrahedron* **2022**, *106*, 132641. [[CrossRef](#)]

18. Pouran, S.R.; Raman, A.A.A.; Daud, W.M.A.W. Review on the Application of Modified Iron Oxides as Heterogeneous Catalysts in Fenton Reactions. *J. Clean. Prod.* **2014**, *64*, 24–35. [[CrossRef](#)]
19. Malhotra, N.; Lee, J.S.; Liman, R.A.D.; Ruallo, J.M.S.; Villaflores, O.B.; Ger, T.R.; Hsiao, C.D. Potential Toxicity of Iron Oxide Magnetic Nanoparticles: A Review. *Molecules* **2020**, *25*, 3159. [[CrossRef](#)]
20. Rusevova, K.; Kopinke, F.D.; Georgi, A. Nano-Sized Magnetic Iron Oxides as Catalysts for Heterogeneous Fenton-Like Reactions—Influence of Fe(II)/Fe(III) Ratio on Catalytic Performance. *J. Hazard. Mater.* **2012**, *241*, 433–440. [[CrossRef](#)]
21. Elahi, N.; Rizwan, M. Progress and Prospects of Magnetic Iron Oxide Nanoparticles in Biomedical Applications: A review. *Artif. Organs* **2021**, *45*, 1272–1299. [[CrossRef](#)] [[PubMed](#)]
22. Vásquez-Céspedes, S.; Betori, R.C.; Cismesia, M.A.; Kirsch, J.K.; Yang, Q. Heterogeneous Catalysis for Cross-Coupling Reactions: An Underutilized Powerful and Sustainable Tool in the Fine Chemical Industry? *Org. Process Res. Dev.* **2021**, *25*, 740–753. [[CrossRef](#)]
23. Srivastava, A.; Kaur, H.; Pahuja, H.; Rangarajan, T.M.; Varma, R.S.; Pasricha, S. Optimal Exploitation of Supported Heterogenized Pd Nanoparticles for C-C Cross-Coupling Reactions. *Coord. Chem. Rev.* **2024**, *507*, 215763. [[CrossRef](#)]
24. Cera, G.; Ackermann, L. Iron-Catalyzed C–H Functionalization Processes. In *Ni- and Fe-Based Cross-Coupling Reactions*; Springer: Berlin/Heidelberg, Germany, 2017; pp. 191–224.
25. Gopalaiah, K. Chiral Iron Catalysts for Asymmetric Synthesis. *Chem. Rev.* **2013**, *113*, 3248–3296. [[CrossRef](#)] [[PubMed](#)]
26. Quintard, A.; Constantieux, T.; Rodriguez, J. An Iron/Amine-Catalyzed Cascade Process for the Enantioselective Functionalization of Allylic Alcohols. *Angew. Chem.* **2013**, *125*, 13121. [[CrossRef](#)]
27. Roy, S.D.; Das, K.C.; Dhar, S.S. Conventional to Green Synthesis of Magnetic Iron Oxide Nanoparticles; Its Application as Catalyst, Photocatalyst and Toxicity: A Short Review. *Inorg. Chem. Commun.* **2021**, *134*, 109050. [[CrossRef](#)]
28. Liu, Y.; You, T.; Wang, H.X.; Tang, Z.; Zhou, C.Y.; Che, C.M. Iron-And Cobalt-Catalyzed C (Sp³)–H Bond Functionalization Reactions and Their Application in Organic Synthesis. *Chem. Soc. Rev.* **2020**, *49*, 5310–5358. [[CrossRef](#)]
29. Zhang, R.K.; Chen, K.; Huang, X.; Wohlschlager, L.; Renata, H.; Arnold, F.H. Enzymatic Assembly of Carbon–Carbon Bonds via Iron-Catalyzed Sp³ C–H Functionalization. *Nature* **2019**, *565*, 67–72. [[CrossRef](#)] [[PubMed](#)]
30. Rogge, T.; Kaplaneris, N.; Chatani, N.; Kim, J.; Chang, S.; Punji, B.; Schafer, L.L.; Musaev, D.G.; Wencel-Delord, J.; Roberts, C.A.; et al. C–H Activation. *Nat. Rev. Methods Prim.* **2021**, *1*, 43. [[CrossRef](#)]
31. Ouyang, X.H.; Li, Y.; Song, R.J.; Hu, M.; Luo, S.; Li, J.H. Intermolecular Dialkylation of Alkenes with Two Distinct C (Sp³)–H Bonds Enabled by Synergistic Photoredox Catalysis and Iron Catalysis. *Sci. Adv.* **2019**, *5*, 9839. [[CrossRef](#)]
32. Bettoni, L.; Seck, C.; Mbaye, M.D.; Gaillard, S.; Renaud, J.L. Iron-Catalyzed Tandem Three-Component Alkylation: Access to α -Methylated Substituted Ketones. *Org. Lett.* **2019**, *21*, 3057–3061. [[CrossRef](#)]
33. Lemmens, V.; Janssens, K.; Baestaens, W.J.; Bugaev, A.L.; Van Velthoven, N.; Adriaensen, K.; Marquez, C.; Henrion, M.; De Vos, D.E. An Iron-Loaded Metal–Organic Framework (CAU-27-Fe) As Effective Heterogeneous Catalyst for The Direct C–H Amination of Ethers Using NH-Heterocycles. *J. Catal.* **2024**, *434*, 115516. [[CrossRef](#)]
34. Liu, Y.; You, T.; Wang, T.T.; Che, C.M. Iron-Catalyzed C–H Amination and Its Application in Organic Synthesis. *Tetrahedron* **2019**, *75*, 130607. [[CrossRef](#)]
35. Du, Y.; Tang, J.J.; Wang, Y.; Hu, J.; Chen, C.; Xiong, Z.; Li, Y.; Fan, J.; Bao, M.; Yu, X. Visible-Light-Driven Iron-Catalyzed Intermolecular Benzylic C (sp³)–H Amination with 1, 2, 3, 4-Tetrazoles. *Org. Lett.* **2024**, *26*, 664–669. [[CrossRef](#)] [[PubMed](#)]
36. Lv, B.; Gao, P.; Zhang, S.; Jia, X.; Wang, M.; Yuan, Y. Iron (iii)-catalyzed direct C–H radical amination of (hetero) arenes. *Org. Chem. Front.* **2021**, *8*, 5440–5445. [[CrossRef](#)]
37. Doan, S.H.; Tran, C.B.; Cao, A.L.; Le, N.T.; Phan, N.T. A New Pathway to 2-Arylbenzoxazoles And 2-Arylbenzothiazoles via One-Pot Oxidative Cyclization Reactions Under Iron–Organic Framework Catalysis. *Catal. Lett.* **2019**, *149*, 2053–2063. [[CrossRef](#)]
38. Zhou, Y.; Ni, J.; Lyu, Z.; Li, Y.; Wang, T.; Cheng, G.J. Mechanism and Reaction Channels of Iron-Catalyzed Primary Amination of Alkenes by Hydroxylamine Reagents. *ACS Catal.* **2023**, *13*, 1863–1874. [[CrossRef](#)]
39. Shang, R.; Ilies, L.; Nakamura, E. Iron-catalyzed C–H bond activation. *Chem. Rev.* **2017**, *117*, 9086–9139. [[CrossRef](#)] [[PubMed](#)]
40. Doba, T.; Shang, R.; Nakamura, E. Iron-Catalyzed C–H Activation for Heterocoupling and Copolymerization of Thiophenes with Enamines. *J. Am. Chem. Soc.* **2022**, *144*, 21692–21701. [[CrossRef](#)]
41. Yoshikai, N.; Nakamura, E. Theoretical Studies on Diastereo- and Enantioselective Rhodium-Catalyzed Cyclization of Diazo Compound via Intramolecular C–H Bond Insertion. *Adv. Synth. Catal.* **2003**, *345*, 1159–1171. [[CrossRef](#)]
42. Nakamura, N.; Tajima, Y.; Sakai, K. Direct Phenylation of Isoxazoles Using Palladium Catalysts. Synthesis of 4-Phenylmuscimol. *Heterocycles* **1982**, *17*, 235. [[CrossRef](#)]
43. Nakamura, E.; Yoshikai, N. Low-Valent Iron-Catalyzed C–C Bond Formation—Addition, Substitution, and C–H Bond Activation. *J. Org. Chem.* **2010**, *75*, 6061–6067. [[CrossRef](#)] [[PubMed](#)]
44. Loup, J.; Dhawa, U.; Pesciaoli, F.; Wencel-Delord, J.; Ackermann, L. Enantioselective C–H Activation with Earth-Abundant 3d Transition Metals. *Angew. Chem. Int. Ed.* **2019**, *58*, 12803–12818. [[CrossRef](#)]
45. Ackermann, L. Metalla-Electrocatalyzed C–H Activation by Earth-Abundant 3d Metals and Beyond. *Acc. Chem. Res.* **2019**, *53*, 84–104. [[CrossRef](#)] [[PubMed](#)]
46. Messinis, A.M.; Finger, L.H.; Hu, L.; Ackermann, L. Allenes for Versatile Iron-Catalyzed C–H Activation by Weak O-Coordination: Mechanistic Insights by Kinetics, Intermediate Isolation, and Computation. *J. Am. Chem. Soc.* **2020**, *142*, 13102–13111. [[CrossRef](#)]

47. Ackermann, L. Carboxylate-Assisted Transition-Metal-Catalyzed C–H Bond Functionalizations: Mechanism and Scope. *Chem. Rev.* **2011**, *11*, 1315–1345. [[CrossRef](#)] [[PubMed](#)]
48. Gandeepan, P.; Muller, T.; Zell, D.; Cera, G.; Warratz, S.; Ackermann, L. 3d Transition Metals for C–H Activation. *Chem. Rev.* **2018**, *119*, 2192–2452. [[CrossRef](#)]
49. Mo, J.; Messinis, A.M.; Li, J.; Warratz, S.; Ackermann, L. Chelation-Assisted Iron-Catalyzed C–H Activations: Scope and Mechanism. *Acc. Chem. Res.* **2023**, *57*, 10–22. [[CrossRef](#)]
50. Cattani, S.; Cera, G. Modern Organometallic C–H Functionalizations with Earth-Abundant Iron Catalysts: An Update. *Chem. Asian J.* **2024**, *19*, e202300897. [[CrossRef](#)]
51. Zhang, L.; Liardet, L.; Luo, J.; Ren, D.; Grätzel, M.; Hu, X. Photo-electrocatalytic arene C–H amination. *Nat. Catal.* **2019**, *2*, 366–373. [[CrossRef](#)]
52. Devarajan, N.; Suresh, P. Iron-MOF-Catalyzed Domino Cyclization and Aromatization Strategy for the Synthesis of 2,4-Diarylquinolines. *Asian J. Org. Chem.* **2020**, *9*, 437–444. [[CrossRef](#)]
53. To, T.A.; Vo, Y.H.; Nguyen, H.T.; Ha, P.T.; Doan, S.H.; Doan, T.L.; Li, S.; Le, H.V.; Tu, T.N.; Phan, N.T. Iron-Catalyzed One-Pot Sequential Transformations: Synthesis of Quinazolinones via Oxidative Csp³H Bond Activation Using a New Metal-Organic Framework as Catalyst. *J. Catal.* **2019**, *370*, 11–20. [[CrossRef](#)]
54. Doan, S.H.; Tran, N.K.; Pham, P.H.; Nguyen, V.H.; Nguyen, N.N.; Ha, P.T.; Li, S.; Le, H.V.; Le, N.T.; Tu, T.N.; et al. A New Synthetic Pathway to Triphenylpyridines via Cascade Reactions Utilizing a New Iron-Organic Framework as a Recyclable Heterogeneous Catalyst. *Eur. J. Org. Chem.* **2019**, *2019*, 2382–2389. [[CrossRef](#)]
55. Motokura, K.; Ozawa, N.; Sato, R.; Manaka, Y.; Chun, W.J. Porous FeO(OH) Dispersed on Mg–Al Hydrotalcite Surface for One-Pot Synthesis of Quinoline Derivatives. *ChemCatChem* **2021**, *13*, 2915–2921. [[CrossRef](#)]
56. Mashhoori, M.S.; Sandaroos, R. New Ecofriendly Heterogeneous Nano-Catalyst for the Synthesis of 1-Substituted and 5-Substituted 1 H-Tetrazole Derivatives. *Sci. Rep.* **2022**, *12*, 15364. [[CrossRef](#)] [[PubMed](#)]
57. Waghchaure, R.H.; Jagdale, B.S.; Koli, P.B.; Adole, V.A. Nano 5% Fe–ZnO: A highly efficient and recyclable heterogeneous solid nano catalyst for the Biginelli reaction. *J Indian Chem. Soc.* **2022**, *99*, 100468. [[CrossRef](#)]
58. Sánchez-Velandia, J.E.; Villa, A.L. Isomerization of α - and β -Pinene Epoxides Over Fe or Cu Supported MCM-41 and SBA-15 Materials. *Appl. Catal. A Gen.* **2019**, *580*, 17–27. [[CrossRef](#)]
59. Fürstner, A.; Leitner, A.; Méndez, M.; Krause, H. Iron-Catalyzed Cross-Coupling Reactions. *J. Am. Chem. Soc.* **2002**, *124*, 13856–13863. [[CrossRef](#)] [[PubMed](#)]
60. Czaplik, W.M.; Mayer, M.; Cvengroš, J.; von Wangelin, A.J. Coming of Age: Sustainable Iron-Catalyzed Cross-Coupling Reactions. *ChemSusChem* **2009**, *2*, 396–417. [[CrossRef](#)]
61. Cassani, C.; Bergonzini, G.; Wallentin, C.J. Active Species and Mechanistic Pathways in Iron-Catalyzed C–C Bond-Forming Cross-Coupling Reactions. *ACS Catal.* **2016**, *6*, 1640–1648. [[CrossRef](#)]
62. Jang, S.; Hira, S.A.; Annas, D.; Song, S.; Yusuf, M.; Park, J.C.; Park, S.; Park, K.H. Recent Novel Hybrid Pd–Fe₃O₄ Nanoparticles as Catalysts for Various C–C Coupling Reactions. *Processes* **2019**, *7*, 422. [[CrossRef](#)]
63. Hegde, S.; Nizam, A.; Vijayan, A. Furaldehyde-Based Magnetic Supported Palladium Nanoparticles as an Efficient Heterogeneous Catalyst for Mizoroki–Heck Cross-Coupling Reaction. *New J. Chem.* **2024**, *48*, 1121–1129. [[CrossRef](#)]
64. Sonawane, S.A.; Mhaldar, P.M.; Chhowala, T.N.; Pore, D.M. Novel Palladium Tagged Ferrite Nanoparticle Supported Ionic Liquid Phase Catalyst for The Efficient Copper-Free Sonogashira Coupling. *J. Mol. Struct.* **2022**, *1269*, 133729. [[CrossRef](#)]
65. Sardarian, A.R.; Eslahi, H.; Esmaeilpour, M. Green, Cost-Effective and Efficient Procedure for Heck and Sonogashira Coupling Reactions Using Palladium Nanoparticles Supported on Functionalized Fe₃O₄@SiO₂ by Polyvinyl Alcohol as a Highly Active, Durable and Reusable Catalyst. *Appl. Organomet. Chem.* **2019**, *33*, e4856. [[CrossRef](#)]
66. Akay, S.; Baran, T.; Kayan, B.; Kalderis, D. Assessment of a Pd–Fe₃O₄-Biochar Nanocomposite as a Heterogeneous Catalyst for the Solvent-Free Suzuki–Miyaura Reaction. *Mater. Chem. Phys.* **2021**, *259*, 124176. [[CrossRef](#)]
67. Tamoradi, T.; Daraie, M.; Heravi, M.M. Synthesis of Palladated Magnetic Nanoparticle (Pd@Fe₃O₄/AMOCOA) as an Efficient and Heterogeneous Catalyst for Promoting Suzuki and Sonogashira Cross-Coupling Reactions. *Appl. Organomet. Chem.* **2020**, *34*, e5538. [[CrossRef](#)]
68. Halligudra, G.; Paramesh, C.C.; Mudike, R.; Ningegowda, M.; Rangappa, D.; Shivaramu, P.D. PdII on Guanidine-Functionalized Fe₃O₄ Nanoparticles as an Efficient Heterogeneous Catalyst for Suzuki–Miyaura Cross-Coupling and Reduction of Nitroarenes in Aqueous Media. *ACS Omega* **2021**, *6*, 34416–34428. [[CrossRef](#)] [[PubMed](#)]
69. Bora, T.J.; Hazarika, N.; Gour, N.K.; Lee, S.; Park, Y.B.; Biswas, S.; Devi, A.; Bania, K.K. Low-Palladium-Content Iron (III) Nanocatalyst Supported on Zeolite-NaY for C–Cl Bond Activation. *ACS Appl. Nano Mater.* **2023**, *6*, 17972–17985. [[CrossRef](#)]
70. Akkoc, M.; Buğday, N.; Altın, S.; Yaşar, S. Magnetite@MCM-41 Nanoparticles as Support Material for Pd–N-Heterocyclic Carbene Complex: A Magnetically Separable Catalyst for Suzuki–Miyaura Reaction. *Appl. Organomet. Chem.* **2021**, *35*, e6233. [[CrossRef](#)]
71. Çalışkan, M.; Baran, T. Decorated Palladium Nanoparticles on Chitosan/ δ -FeOOH Microspheres: A Highly Active and Recyclable Catalyst for Suzuki Coupling Reaction and Cyanation of Aryl Halides. *Int. J. Biol. Macromol.* **2021**, *174*, 120–133. [[CrossRef](#)]
72. Sheikh, S.; Nasser, M.A.; Chahkandi, M.; Reiser, O.; Allahresani, A. Dendritic structured Palladium Complexes: Magnetically Retrievable, Highly Efficient Heterogeneous Nanocatalyst for Suzuki and Heck Cross-Coupling Reactions. *RSC Adv.* **2022**, *12*, 8833–8840. [[CrossRef](#)]

73. Vibhute, S.P.; Mhaldar, P.M.; Shejwal, R.V.; Pore, D.M. Magnetic nanoparticles-supported palladium catalyzed Suzuki-Miyaura cross coupling. *Tetrahedron Lett.* **2020**, *61*, 151594. [[CrossRef](#)]
74. Baran, T.; Nasrollahzadeh, M. Facile Fabrication of Magnetically Separable Palladium Nanoparticles Supported on Modified Kaolin as a Highly Active Heterogeneous Catalyst for Suzuki Coupling Reactions. *J. Phys. Chem. Solids* **2020**, *146*, 109566. [[CrossRef](#)]
75. Liu, B.; Yan, Z.; Xu, T.; Li, C.; Gao, R.; Hao, H.; Bai, J. Co-Construction of Oxygen Vacancies and Heterojunctions on CeO₂ via One-Step Fe Doping for Enhanced Photocatalytic Activity in Suzuki Reaction. *Chem. Eng. J.* **2022**, *442*, 136226. [[CrossRef](#)]
76. Jahanshahi, R.; Khazaei, A.; Sobhani, S.; Sansano, J.M. gC₃N₄/γ-Fe₂O₃/TiO₂/Pd: A New Magnetically Separable Photocatalyst for Visible-Light-Driven Fluoride-Free Hiyama and Suzuki–Miyaura Cross-Coupling Reactions at Room Temperature. *New J. Chem.* **2020**, *44*, 11513–11526. [[CrossRef](#)]
77. Adam, M.S.S.; Ullah, F.; Makhlof, M.M. Hybrid Organic-Inorganic Cu(II) Iminoisonicotine@TiO₂@Fe₃O₄ Heterostructure as Efficient Catalyst for Cross-Couplings. *J. Am. Ceram. Soc.* **2020**, *103*, 4632–4653. [[CrossRef](#)]
78. Deepa, M.; Selvarasu, U.; Kalaivani, K.; Parasuraman, K. Recyclable Heterogeneous Iron Supported on Imidazolium Ionic Liquid Catalysed Palladium and Copper-Free Heck Reaction. *J. Organomet. Chem.* **2021**, *954*, 122073. [[CrossRef](#)]
79. Hajipour, A.R.; Abolfathi, P.; Tavangar-Rizi, Z. Iron-catalyzed cross-coupling reaction: Heterogeneous palladium and copper-free Heck and Sonogashira cross-coupling reactions catalyzed by a reusable Fe (III) complex. *Appl. Organomet. Chem.* **2018**, *32*, e4353. [[CrossRef](#)]
80. Min, Q.; Miao, P.; Chu, D.; Liu, J.; Qi, M.; Kazemnejadi, M. Introduction of a Recyclable Basic Ionic Solvent with Bis-(NHC) Ligand Property and the Possibility of Immobilization on Magnetite for Ligand-And Base-Free Pd-Catalyzed Heck, Suzuki and Sonogashira Cross-Coupling Reactions in Water. *Catal. Lett.* **2021**, *151*, 3030–3047. [[CrossRef](#)]
81. Sobhani, S.; Esmailzadeh-Soleimani, S. Immobilized Palladium-Pyridine Complex On γ-Fe₂O₃ Magnetic Nanoparticles as a New Magnetically Recyclable Heterogeneous Catalyst for Heck, Suzuki and Copper-Free Sonogashira Reactions. *Org. Chem. Res.* **2019**, *5*, 10–24.
82. Tashrifi, Z.; Bahadorikhalili, S.; Lijan, H.; Ansari, S.; Hamedifar, H.; Mahdavi, M. Synthesis and Characterization of γ-Fe₂O₃@SiO₂-(CH₂)₃-PDTC-Pd Magnetic Nanoparticles: A New and Highly Active Catalyst for the Heck/Sonogashira Coupling Reactions. *New J. Chem.* **2019**, *43*, 8930–8938. [[CrossRef](#)]
83. Kazemnejadi, M.; Rezazadeh, Z.; Nasseri, M.A.; Allahresani, A.; Esmailpour, M. Imidazolium Chloride-Co (III) Complex Immobilized on Fe₃O₄@SiO₂ as a Highly Active Bifunctional Nanocatalyst for the Copper-, Phosphine-, and Base-Free Heck and Sonogashira Reactions. *Green Chem.* **2019**, *21*, 1718–1734. [[CrossRef](#)]
84. Gebbink, R.J.K.; Moret, M.E. (Eds.) *Non-Noble Metal Catalysis: Molecular Approaches and Reactions*; John Wiley & Sons: Hoboken, NJ, USA, 2019.
85. Muci, A.R.; Buchwald, S.L. Practical palladium catalysts for CN and CO bond formation. In *Cross-Coupling Reactions: A Practical Guide*; Springer: Berlin/Heidelberg, Germany, 2002; pp. 131–209.
86. Sun, Y.; Tang, H.; Chen, K.; Hu, L.; Yao, J.; Shaik, S.; Chen, H. Two-State Reactivity in Low-Valent Iron-Mediated C–H Activation and the Implications for Other First-Row Transition Metals. *J. Am. Chem. Soc.* **2016**, *138*, 3715–3730. [[CrossRef](#)]
87. Aoki, Y.; Toyoda, T.; Kawasaki, H.; Takaya, H.; Sharma, A.K.; Morokuma, K.; Nakamura, M. Iron-Catalyzed Chemoselective C–N Coupling Reaction: A Protecting-Group-Free Amination of Aryl Halides Bearing Amino or Hydroxy Groups. *Asian J. Org. Chem.* **2020**, *9*, 372–376. [[CrossRef](#)]
88. Kaviani, N.; Behrouz, S.; Jafari, A.A.; Rad, M.N.S. Functionalization of Fe₃O₄@SiO₂ Nanoparticles with Cu (I)-Thiosemicarbazone Complex as a Robust and Efficient Heterogeneous Nanocatalyst for N-Arylation of N-Heterocycles with Aryl Halides. *RSC Adv.* **2023**, *13*, 30293–30305. [[CrossRef](#)] [[PubMed](#)]
89. Chahkamali, F.O.; Sobhani, S.; Sansano, J.M. Water-Dispersible Pd–N-Heterocyclic Carbene Complex Immobilized on Magnetic Nanoparticles as a New Heterogeneous Catalyst for Fluoride-Free Hiyama, Suzuki–Miyaura and Cyanation Reactions in Aqueous Media. *Catal. Lett.* **2022**, *152*, 2650–2668. [[CrossRef](#)]
90. Abdollahi-Alibeik, M.; Ramazani, Z. Synthesis, Characterization and Application of Magnetic Mesoporous Fe₃O₄@Fe-Cu/MCM-41 as Efficient and Recyclable Nanocatalyst for the Buchwald-Hartwig CN Cross-Coupling Reaction. *J. Chem. Sci.* **2022**, *134*, 77. [[CrossRef](#)]
91. Nithya, K.; Anbarasan, R.; Anbuselvan, N.; Vasantha, V.S.; Suresh, D.; Amali, A.J. Heterogenization of Cobalt on Nanostructured Magnetic Covalent Triazine Framework: Effective Catalyst for Buchwald-Hartwig N-Arylation, Reduction, and Oxidation Reactions. *ACS Appl. Nano Mater.* **2024**, *7*, 9554–9564. [[CrossRef](#)]
92. Zhang, W.; Veisi, H.; Sharifi, R.; Salamat, D.; Karmakar, B.; Hekmati, M.; Hemmati, S.; Zangeneh, M.M.; Zhang, Z.; Su, Q. Fabrication of Pd NPs on Pectin-Modified Fe₃O₄ NPs: A Magnetically Retrievable Nanocatalyst for Efficient C–C and C–N Cross Coupling Reactions and an Investigation of its Cardiovascular Protective Effects. *Int. J. Biol. Macromol.* **2020**, *160*, 1252–1262. [[CrossRef](#)]
93. Rouzifar, M.; Sobhani, S.; Farrokhi, A.; Sansano, J.M. Fe-MIL-101 Modified by Isatin-Schiff-Base-Co: A Heterogeneous Catalyst for C–C, C–O, C–N, and C–P Cross Coupling Reactions. *New J. Chem.* **2021**, *45*, 19963–19976. [[CrossRef](#)]
94. Dubey, A.V.; Kumar, A.V. A Bio-Inspired Magnetically Recoverable Palladium Nanocatalyst for the Ullmann Coupling reaction of Aryl halides and Arylboronic acids In Aqueous Media. *Appl. Organomet. Chem.* **2020**, *34*, e5570. [[CrossRef](#)]

95. Fekri, S.; Mansoori, Y.; Esquivel, D.; Navarro, M.A. A New Bis-(NHC)-P (II) Complex Supported on Magnetic Mesoporous Silica: An Efficient Pd (II) Catalyst for the Selective Buchwald-Hartwig Monoarylation of Ammonia. *ChemistrySelect* **2023**, *8*, e202204378. [[CrossRef](#)]
96. Hemmati, S.; Ahany Kamangar, S.; Yousefi, M.; Hashemi Salehi, M.; Hekmati, M. Cu (I)-Anchored Polyvinyl Alcohol Coated-Magnetic Nanoparticles as Heterogeneous Nanocatalyst in Ullmann-Type C–N Coupling Reactions. *Appl. Organomet. Chem.* **2020**, *34*, e5611. [[CrossRef](#)]
97. Ding, Q.; Yu, Y.; Huang, F.; Zhang, L.; Zheng, J.G.; Xu, M.; Baell, J.B.; Huang, H. A Reusable CNT-Supported Single-Atom Iron Catalyst for the Highly Efficient Synthesis of C–N Bonds. *Chem. Eur. J.* **2020**, *26*, 4592–4598. [[CrossRef](#)] [[PubMed](#)]
98. Sun, K.; Shan, H.; Neumann, H.; Lu, G.P.; Beller, M. Efficient Iron Single-Atom Catalysts for Selective Ammoxidation of Alcohols to Nitriles. *Nat. Commun.* **2022**, *13*, 1848. [[CrossRef](#)] [[PubMed](#)]
99. Wu, J.; Darcel, C. Iron-Catalyzed Hydrogen Transfer Reduction of Nitroarenes with Alcohols: Synthesis of Imines and AZA Heterocycles. *J. Org. Chem.* **2020**, *86*, 1023–1036. [[CrossRef](#)] [[PubMed](#)]
100. Podyacheva, E.; Afanasyev, O.I.; Vasilyev, D.V.; Chusov, D. Borrowing Hydrogen Amination Reactions: A Complex Analysis of Trends and Correlations of the Various Reaction Parameters. *ACS Catal.* **2022**, *12*, 7142–7198. [[CrossRef](#)]
101. Coutanceau, C.; Brimaud, S.; Lamy, C.; Léger, J.M.; Dubau, L.; Rousseau, S.; Vigier, F. Review of Different Methods for Developing Nanoelectrocatalysts for the Oxidation of Organic Compounds. *Electrochim. Acta* **2008**, *53*, 6865–6880. [[CrossRef](#)]
102. Xiong, L.; Tang, J. Strategies and Challenges on Selectivity of Photocatalytic Oxidation of Organic Substances. *Adv. Energy Mater.* **2021**, *11*, 2003216. [[CrossRef](#)]
103. Ma, D.; Yi, H.; Lai, C.; Liu, X.; Huo, X.; An, Z.; Li, L.; Fu, Y.; Li, B.; Zhang, M.; et al. Critical Review of Advanced Oxidation Processes in Organic Wastewater Treatment. *Chemosphere* **2021**, *275*, 130104. [[CrossRef](#)]
104. Luo, H.; Zeng, Y.; He, D.; Pan, X. Application of Iron-Based Materials in Heterogeneous Advanced Oxidation Processes for Wastewater Treatment: A Review. *Chem. Eng. J.* **2021**, *407*, 127191. [[CrossRef](#)]
105. Liu, J.; Peng, C.; Shi, X. Preparation, characterization, and applications of Fe-based catalysts in advanced oxidation processes for organics removal: A review. *Environ. Pollut.* **2022**, *293*, 118565. [[CrossRef](#)] [[PubMed](#)]
106. Esteves, B.M.; Morales-Torres, S.; Maldonado-Hódar, F.J.; Madeira, L.M. Fitting Biochars and Activated Carbons from Residues of the Olive Oil Industry as Supports of Fe-Catalysts for the Heterogeneous Fenton-Like Treatment of Simulated Olive Mill Wastewater. *Nanomaterials* **2020**, *10*, 876. [[CrossRef](#)] [[PubMed](#)]
107. Peng, L.; Duan, X.; Shang, Y.; Gao, B.; Xu, X. Engineered Carbon Supported Single Iron Atom Sites and Iron Clusters from Fe-Rich Enteromorpha for Fenton-Like Reactions via Nonradical Pathways. *Appl. Catal. B Environ.* **2021**, *287*, 119963. [[CrossRef](#)]
108. Madihi-Bidgoli, S.; Asadnezhad, S.; Yaghoot-Nezhad, A.; Hassani, A. Azurobine Degradation Using Fe₂O₃@Multi-Walled Carbon Nanotube Activated Peroxymonosulfate (PMS) Under UVA-LED Irradiation: Performance, Mechanism and Environmental Application. *J. Environ. Chem. Eng.* **2021**, *9*, 106660. [[CrossRef](#)]
109. Chen, L.; Wang, S.; Yang, Z.; Qian, J.; Pan, B. Selective Interfacial Oxidation of Organic Pollutants in Fenton-Like System Mediated by Fe(III)-Adsorbed Carbon Nanotubes. *Appl. Catal. B Environ.* **2021**, *292*, 120193. [[CrossRef](#)]
110. Xie, A.; Cui, J.; Yang, J.; Chen, Y.; Lang, J.; Li, C.; Yan, Y.; Dai, J. Graphene oxide/Fe (III)-Based Metal-Organic Framework Membrane for Enhanced Water Purification Based on Synergistic Separation and Photo-Fenton Processes. *Appl. Catal. B Environ.* **2020**, *264*, 118548. [[CrossRef](#)]
111. Pervez, M.N.; He, W.; Zarra, T.; Naddeo, V.; Zhao, Y. New Sustainable Approach for The Production of Fe₃O₄/Graphene Oxide-Activated Persulfate System for Dye Removal in Real Wastewater. *Water* **2020**, *12*, 733. [[CrossRef](#)]
112. Görmez, F.; Görmez, Ö.; Gözmen, B.; Kalderis, D. Degradation of Chloramphenicol and Metronidazole by Electro-Fenton Process Using Graphene Oxide-Fe₃O₄ as Heterogeneous Catalyst. *J. Environ. Chem. Eng.* **2019**, *7*, 102990. [[CrossRef](#)]
113. Le, T.X.H.; Drobek, M.; Bechelany, M.; Motuzas, J.; Julbe, A.; Cretin, M. Application of Fe-MFI Zeolite Catalyst in Heterogeneous Electro-Fenton Process for Water Pollutants Abatement. *Micropor. Mesopor. Mater.* **2019**, *278*, 64–69.
114. Chan-Thaw, C.E.; Savara, A.; Villa, A. Selective Benzyl Alcohol Oxidation Over Pd Catalysts. *Catalysts* **2018**, *8*, 431. [[CrossRef](#)]
115. Ferguson, L.N. The synthesis of aromatic aldehydes. *Chem. Rev.* **1946**, *38*, 227–254. [[CrossRef](#)]
116. Jacquot, C.; Middelkoop, V.; Köckritz, A.; Pohar, A.; Bienert, R.; Kellici, S.; Bărăgău, I.A.; Venezia, B.; Gavriilidis, A.; Likozer, B.; et al. 3D Printed Catalytic Reactors for Aerobic Selective Oxidation of Benzyl Alcohol into Benzaldehyde in Continuous Multiphase Flow. *Sustain. Mater. Technol.* **2021**, *30*, e00329. [[CrossRef](#)]
117. Wang, Z.; Shi, J.; Wang, D.; Pu, Y.; Wang, J.X.; Chen, J.F. Metal-free catalytic oxidation of benzylic alcohols for benzaldehyde. *React. Chem. Eng.* **2019**, *4*, 507–515. [[CrossRef](#)]
118. Crombie, C.M.; Lewis, R.J.; Taylor, R.L.; Morgan, D.J.; Davies, T.E.; Folli, A.; Murphy, D.M.; Edwards, J.K.; Qi, J.; Jiang, H.; et al. Enhanced Selective Oxidation of Benzyl Alcohol via in Situ H₂O₂ Production Over Supported Pd-Based Catalysts. *ACS Catal.* **2021**, *11*, 2701–2714. [[CrossRef](#)]
119. Das, B.; Baruah, M.J.; Sharma, M.; Sarma, B.; Karunakar, G.V.; Satyanarayana, L.; Roy, S.; Bhattacharyya, P.K.; Borah, K.K.; Bania, K.K. Self pH Regulated Iron (II) Catalyst for Radical Free Oxidation of Benzyl Alcohols. *Appl. Catal. A Gen.* **2020**, *589*, 117292. [[CrossRef](#)]
120. Iraqui, S.; Kashyap, S.S.; Rashid, M.H. NiFe₂O₄ Nanoparticles: An Efficient and Reusable Catalyst for the Selective Oxidation of Benzyl Alcohol to Benzaldehyde Under Mild Conditions. *Nanoscale Adv.* **2020**, *2*, 5790–5802. [[CrossRef](#)]

121. Baruah, M.J.; Bora, T.J.; Dutta, R.; Roy, S.; Guha, A.K.; Bania, K.K. Fe (III) Superoxide Radicals in Halloysite Nanotubes for Visible-Light-Assisted Benzyl Alcohol Oxidation and Oxidative C-C Coupling of 2-Naphthol. *Mol. Catal.* **2021**, *515*, 111858. [[CrossRef](#)]
122. Wei, Q.; Wang, J.; Shen, W. Atomically Dispersed Fe^{δ+} Anchored on Nitrogen-Rich Carbon for Enhancing Benzyl Alcohol Oxidation Through Mott-Schottky Effect. *Appl. Catal. B Environ.* **2021**, *292*, 120195. [[CrossRef](#)]
123. Correia, L.M.; Kuznetsov, M.L.; Alegria, E.C. Core-Shell Catalysts for Conventional Oxidation of Alcohols: A Brief Review. *Catalysts* **2023**, *13*, 1137. [[CrossRef](#)]
124. Sun, L.; Zhan, W.; Shang, J.; Chen, G.; Wang, S.; Chen, Y.; Long, Z. Carbon-Encapsulated Fe₃O₄ for Catalyzing the Aerobic Oxidation of Benzyl Alcohol and Benzene. *React. Kinet. Mech. Catal.* **2019**, *126*, 1055–1065. [[CrossRef](#)]
125. Dabiri, M.; Nikbakht, R.; Movahed, S.K. Palladium Nanoparticle Supported on Core-Shell Fe_x@Nitrogen-Doped Carbon Cubes and Their Photocatalytic Activities in Selective Oxidation of Alcohols and Ullmann Homocoupling in One Reaction System. *Mater. Chem. Phys.* **2021**, *258*, 123908. [[CrossRef](#)]
126. Xu, B.; Senthilkumar, S.; Zhong, W.; Shen, Z.; Lu, C.; Liu, X. Magnetic Core-Shell Fe₃O₄@Cu₂O and Fe₃O₄@Cu₂O-Cu Materials as Catalysts for Aerobic Oxidation of Benzylic Alcohols Assisted by TEMPO and N-Methylimidazole. *RSC Adv.* **2020**, *10*, 26142–26150. [[CrossRef](#)]
127. Paul, A.; Bhuyan, B.; Dhar, S.S. Study of Core-Shell α-Fe₂O₃@Au Nanohybrid and Their High Catalytic Performances in Aerial Oxidation of Benzyl Alcohols. *Chem. Eng. Commun.* **2020**, *207*, 1185–1195. [[CrossRef](#)]
128. Zheng, Z.; Han, F.; Xing, B.; Han, X.; Li, B. Synthesis of Fe₃O₄@CdS@CQDs Ternary Core-Shell Heterostructures as A Magnetically Recoverable Photocatalyst for Selective Alcohol Oxidation Coupled with H₂O₂ Production. *J. Colloid Interface Sci.* **2022**, *624*, 460–470. [[CrossRef](#)] [[PubMed](#)]
129. Malko, D.; Guo, Y.; Jones, P.; Britovsek, G.; Kucernak, A. Heterogeneous Iron Containing Carbon Catalyst (Fe-N/C) for Epoxidation with Molecular Oxygen. *J. Catal.* **2019**, *370*, 357–363. [[CrossRef](#)]
130. Yu, D.; Gao, W.; Xing, S.; Lian, L.; Zhang, H.; Wang, X. Fe-Doped H₃PMo₁₂O₄₀ Immobilized on Covalent Organic Frameworks (Fe/PMA@Cofs): A Heterogeneous Catalyst for the Epoxidation of Cyclooctene with H₂O₂. *RSC Adv.* **2019**, *9*, 4884–4891. [[CrossRef](#)]
131. Rayati, S.; Nafarieh, P. A Practical Innovative Method for Highly Selective Oxidation of Alkenes and Alkanes Using Fe (III) And Mn (III) Porphyrins Supported onto Multi-Wall Carbon Nanotubes as Reusable Heterogeneous Catalysts. *Appl. Organomet. Chem.* **2019**, *33*, e4789. [[CrossRef](#)]
132. Zarnegaryan, A.; Dehbanipour, Z. Iron (II) Complex Supported on Graphene Nanosheet: An Efficient and Heterogeneous Catalyst for Epoxidation of Alkenes. *Appl. Surf. Sci. Adv.* **2021**, *4*, 100074. [[CrossRef](#)]
133. Mitra, M.; Cusso, O.; Bhat, S.S.; Sun, M.; Cianfanelli, M.; Costas, M.; Nordlander, E. Highly Enantioselective Epoxidation of Olefins by H₂O₂ Catalyzed by A Non-Heme Fe (II) Catalyst of A Chiral Tetradentate Ligand. *Dalton Trans.* **2019**, *48*, 6123–6131. [[CrossRef](#)]
134. Solé-Daura, A.; Zhang, T.; Fouilloux, H.; Robert, C.; Thomas, C.M.; Chamoreau, L.M.; Carbó, J.J.; Proust, A.; Guillemot, G.; Poblet, J.M. Catalyst Design for Alkene Epoxidation by Molecular Analogues of Heterogeneous Titanium-Silicalite Catalysts. *ACS Catal.* **2020**, *10*, 4737–4750. [[CrossRef](#)]
135. Li, W.; Wu, G.; Hu, W.; Dang, J.; Wang, C.; Weng, X.; Da Silva, I.; Manuel, P.; Yang, S.; Guan, N.; et al. Direct Propylene Epoxidation with Molecular Oxygen Over Cobalt-Containing Zeolites. *J. Am. Chem. Soc.* **2022**, *144*, 4260–4268. [[CrossRef](#)]
136. Xiong, W.; Gu, X.K.; Zhang, Z.; Chai, P.; Zang, Y.; Yu, Z.; Li, D.; Zhang, H.; Liu, Z.; Huang, W. Fine Cubic Cu₂O Nanocrystals as Highly Selective Catalyst for Propylene Epoxidation with Molecular Oxygen. *Nat. Commun.* **2021**, *12*, 5921. [[CrossRef](#)] [[PubMed](#)]
137. Yang, Z.; Zhang, S.; Zhao, H.; Li, A.; Luo, L.; Guo, L. Subnano-FeO_x Clusters Anchored in an Ultrathin Amorphous Al₂O₃ Nanosheet for Styrene Epoxidation. *ACS Catal.* **2021**, *11*, 11542–11550. [[CrossRef](#)]
138. Xiong, Y.; Sun, W.; Xin, P.; Chen, W.; Zheng, X.; Yan, W.; Zheng, L.; Dong, J.; Zhang, J.; Wang, D.; et al. Gram-Scale Synthesis of High-Loading Single-Atomic-Site Fe Catalysts for Effective Epoxidation of Styrene. *Adv. Mater.* **2020**, *32*, 2000896. [[CrossRef](#)]
139. Pó, R.; Cardi, N. Synthesis of Syndiotactic Polystyrene: Reaction Mechanisms and Catalysis. *Prog. Polym. Sci.* **1996**, *21*, 47–88. [[CrossRef](#)]
140. Niu, C.; Du, K.; Xu, Z.; Li, Z.; Li, T.; Wang, R. Mechanical properties of epoxy resin composites modified by epoxy styrene-butadiene latex. *J. Appl. Polymer Sci.* **2023**, *140*, e54002. [[CrossRef](#)]
141. Wu, L.; Wang, X.; Li, B. Porous Core-Shell Fe₃O₄@CuSiO₃ Microsphere as Effective Catalyst for Styrene Epoxidation. *Appl. Surf. Sci.* **2022**, *591*, 153158. [[CrossRef](#)]
142. Liu, J.; Meng, R.; Li, J.; Jian, P.; Wang, L.; Jian, R. Achieving High-Performance for Catalytic Epoxidation of Styrene with Uniform Magnetically Separable CoFe₂O₄ Nanoparticles. *Appl. Catal. B Environ.* **2019**, *254*, 214–222. [[CrossRef](#)]
143. Sheng, B.; Deng, C.; Li, Y.; Xie, S.; Wang, Z.; Sheng, H.; Zhao, J. In situ hydroxylation of a single-atom iron catalyst for preferential ¹O₂ production from H₂O₂. *ACS Catal.* **2022**, *12*, 14679–14688. [[CrossRef](#)]
144. ElMetwally, A.E.; Eshaq, G.; Yehia, F.Z.; Al-Sabagh, A.M.; Kegnæs, S. Iron Oxychloride as an Efficient Catalyst for Selective Hydroxylation of Benzene to Phenol. *ACS Catal.* **2018**, *8*, 10668–10675. [[CrossRef](#)]
145. Yan, Y.; Wu, J.; Hu, G.; Gao, C.; Guo, L.; Chen, X.; Liu, L.; Song, W. Current State and Future Perspectives of Cytochrome P450 Enzymes for C-H And C=C Oxygenation. *Synth. Systems Biotechnol.* **2022**, *7*, 887–899. [[CrossRef](#)]

146. Cheng, L.; Wang, H.; Cai, H.; Zhang, J.; Gong, X.; Han, W. Iron-Catalyzed Arene C–H Hydroxylation. *Science* **2021**, *374*, 77–81. [[CrossRef](#)]
147. Vega, G.; Quintanilla, A.; Belmonte, M.; Casas, J.A. Kinetic Study of Phenol Hydroxylation by H₂O₂ In 3D Fe/SiC Honeycomb Monolithic Reactors: Enabling the Sustainable Production of Dihydroxybenzenes. *Chem. Eng. J.* **2022**, *428*, 131128. [[CrossRef](#)]
148. Yang, B.; Zhang, S.; Gao, Y.; Huang, L.; Yang, C.; Hou, Y.; Zhang, J. Unique functionalities of carbon shells coating on ZnFe₂O₄ for enhanced photocatalytic hydroxylation of benzene to phenol. *Appl. Catal. B Environ.* **2022**, *304*, 120999. [[CrossRef](#)]
149. Mishra, S.; Bal, R.; Dey, R.K. Heterogeneous Recyclable Copper Oxide Supported on Activated Red Mud as An Efficient and Stable Catalyst for the One Pot Hydroxylation of Benzene to Phenol. *Mol. Catal.* **2021**, *499*, 111310. [[CrossRef](#)]
150. Salazar-Aguilar, A.D.; Vega, G.; Casas, J.A.; Vega-Díaz, S.M.; Tristan, F.; Meneses-Rodríguez, D.; Belmonte, M.; Quintanilla, A. Direct Hydroxylation of Phenol to Dihydroxybenzenes by H₂O₂ and Fe-Based Metal-Organic Framework Catalyst at Room Temperature. *Catalysts* **2020**, *10*, 172. [[CrossRef](#)]
151. Wu, Y.; Zhang, X.; Wang, F.; Zhai, Y.; Cui, X.; Lv, G.; Jiang, T.; Hu, J. Synergistic Effect Between Fe and Cu Species on Mesoporous Silica for Hydroxylation of Benzene to Phenol. *Ind. Eng. Chem. Res.* **2021**, *60*, 8386–8395. [[CrossRef](#)]
152. Yue, M.; Jiang, X.; Zhang, H.; Zhang, S.; Xue, T.; Li, Y. Quasi-solid-phase synthesis of Fe-MFI zeolites by using Fe-containing zeolite seed sol for hydroxylation of benzene with H₂O₂. *Micropor. Mesopor. Mater.* **2020**, *294*, 109891. [[CrossRef](#)]
153. Xiao, P.; Osuga, R.; Wang, Y.; Kondo, J.N.; Yokoi, T. Bimetallic Fe–Cu/β zeolite catalysts for direct hydroxylation of benzene to phenol: Effect of the sequence of ion exchange for Fe and Cu cations. *Catal. Sci. Technol.* **2020**, *10*, 6977–6986. [[CrossRef](#)]
154. Lu, E.; Wu, J.; Yang, B.; Yu, D.; Yu, Z.; Hou, Y.; Zhang, J. Selective hydroxylation of benzene to phenol over Fe nanoparticles encapsulated within N-doped carbon shells. *ACS Appl. Nano Mater.* **2020**, *3*, 9192–9199. [[CrossRef](#)]
155. Zeng, L.; Liang, H.; An, P.; Yu, D.; Yang, C.; Hou, Y.; Zhang, J. Carbon Encapsulated Bimetallic FeCo Nanoalloys for One-Step Hydroxylation of Benzene to Phenol. *Appl. Catal. A Gen.* **2022**, *633*, 118499. [[CrossRef](#)]
156. Yuan, Y.; Yang, J.; Lei, A. Recent Advances in Electrochemical Oxidative Cross-Coupling with Hydrogen Evolution Involving Radicals. *Chem. Soc. Rev.* **2021**, *50*, 10058–10086. [[CrossRef](#)] [[PubMed](#)]
157. Liu, C.; Yuan, J.; Gao, M.; Tang, S.; Li, W.; Shi, R.; Lei, A. Oxidative Coupling Between Two Hydrocarbons: An Update of Recent C–H Functionalizations. *Chem. Rev.* **2015**, *115*, 12138–12204. [[CrossRef](#)] [[PubMed](#)]
158. Shi, W.; Liu, C.; Lei, A. Transition-metal catalyzed oxidative cross-coupling reactions to form C–C bonds involving organometallic reagents as nucleophiles. *Chem. Soc. Rev.* **2011**, *40*, 2761–2776. [[CrossRef](#)]
159. Oheix, E.; Herrero, C.; Moutet, J.; Rebilly, J.N.; Cordier, M.; Guillot, R.; Bourcier, S.; Banse, F.; Sénéchal-David, K.; Auffrant, A. Fe^{III} and Fe^{II} Phosphasalen Complexes: Synthesis, Characterization, and Catalytic Application for 2-Naphthol Oxidative Coupling. *Chem. Eur. J.* **2020**, *26*, 13634–13643. [[CrossRef](#)] [[PubMed](#)]
160. Wang, H. Recent Advances in Asymmetric Oxidative Coupling of 2-Naphthol and Its Derivatives. *Chirality* **2010**, *22*, 827–837. [[CrossRef](#)] [[PubMed](#)]
161. Tkachenko, N.V.; Bryliakov, K.P. Transition metal catalyzed aerobic asymmetric coupling of 2-naphthols. *Mini-Rev. Org. Chem.* **2019**, *16*, 392–398. [[CrossRef](#)]
162. Wu, L.Y.; Usman, M.; Liu, W.B. Enantioselective Iron/Bisquinolyldiamine Ligand-Catalyzed Oxidative Coupling Reaction of 2-Naphthols. *Molecules* **2020**, *25*, 852. [[CrossRef](#)]
163. Horibe, T.; Nakagawa, K.; Hazeyama, T.; Takeda, K.; Ishihara, K. An Enantioselective Oxidative Coupling Reaction of 2-Naphthol Derivatives Catalyzed by Chiral Diphosphine Oxide–Iron (II) Complexes. *Chem. Commun.* **2019**, *55*, 13677–13680. [[CrossRef](#)]
164. Deshpande, N.; Parulkar, A.; Joshi, R.; Diep, B.; Kulkarni, A.; Brunelli, N.A. Epoxide Ring Opening with Alcohols Using Heterogeneous Lewis Acid Catalysts: Regioselectivity and Mechanism. *J. Catal.* **2019**, *370*, 46–54. [[CrossRef](#)]
165. Tadiello, L.; Gandini, T.; Stadler, B.M.; Tin, S.; Jiao, H.; de Vries, J.G.; Pignataro, L.; Gennari, C. Regiodivergent Reductive Opening of Epoxides by Catalytic Hydrogenation Promoted by a (Cyclopentadienone) Iron Complex. *ACS Catal.* **2021**, *12*, 235–246. [[CrossRef](#)]
166. Meng, Y.; Taddeo, F.; Aguilera, A.F.; Cai, X.; Russo, V.; Tolvanen, P.; Leveneur, S. The Lord of the Chemical Rings: Catalytic Synthesis of Important Industrial Epoxide Compounds. *Catalysts* **2021**, *11*, 765. [[CrossRef](#)]
167. Cao, H.; Liu, S.; Wang, X. Environmentally Benign Metal Catalyst for The Ring-Opening Copolymerization of Epoxide and CO₂: State-Of-the-Art, Opportunities, and Challenges. *Green Chem. Eng.* **2022**, *3*, 111–124. [[CrossRef](#)]
168. Della Monica, F.; Buonerba, A.; Capacchione, C. Homogeneous Iron Catalysts in The Reaction of Epoxides with Carbon Dioxide. *Adv. Synth. Catal.* **2019**, *361*, 265–282. [[CrossRef](#)]
169. Das, S.; Asefa, T. Epoxide Ring-Opening Reactions with Mesoporous Silica-Supported Fe (III) Catalysts. *ACS Catal.* **2011**, *1*, 502–510. [[CrossRef](#)]
170. Liu, W.; Li, W.; Spannenberg, A.; Junge, K.; Beller, M. Iron-Catalysed Regioselective Hydrogenation of Terminal Epoxides to Alcohols Under Mild Conditions. *Nat. Catal.* **2019**, *2*, 523–528. [[CrossRef](#)]
171. Shi, J.; Wang, S.; Wang, M.; Wang, X.; Li, W. Robust Salen-Typed Ce-Mofs Supported Fe (III) Catalyst Fabricated by Metalloligand Strategy for Catalytic Epoxides with Alcohols. *Mol. Catal.* **2022**, *533*, 112764. [[CrossRef](#)]
172. Li, Z.; Yan, Y.; Liu, M.; Qu, Z.; Yue, Y.; Mao, T.; Zhao, S.; Liu, M.; Lin, Z. Robust Ring-Opening Reaction via Asymmetrically Coordinated Fe Single Atoms Scaffolded by Spoke-Like Mesoporous Carbon Nanospheres. *Proc. Natl. Acad. Sci. USA* **2023**, *120*, e2218261120. [[CrossRef](#)]

173. Reis, N.V.; Deacy, A.C.; Rosetto, G.; Durr, C.B.; Williams, C.K. Heterodinuclear Mg (II) M (II)(M=Cr, Mn, Fe, Co, Ni, Cu and Zn) complexes for the ring opening copolymerization of carbon dioxide/epoxide and anhydride/epoxide. *Chem. Eur. J.* **2022**, *28*, e202104198. [[CrossRef](#)]
174. Nagarjun, N.; Concepcion, P.; Dhakshinamoorthy, A. MIL-101 (Fe) as an Active Heterogeneous Solid Acid Catalyst for the Regioselective Ring Opening of Epoxides by Indoles. *Mol. Catal.* **2020**, *482*, 110628. [[CrossRef](#)]
175. Shi, X.L.; Sun, B.; Hu, Q.; Chen, Y.; Duan, P. Fiber-Supported Fe (III) Complex Catalyst in Spinning Basket Reactor for Cleaner Ring-Opening of Epoxides with Alcohols. *Green Chem.* **2019**, *21*, 3573–3582. [[CrossRef](#)]
176. Wang, D.; Yang, Y.; Zhang, F.; Jiang, P.; Gao, W.; Cong, R.; Yang, T. Ring-Opening Hydration of Epoxides into Diols with a Low Water–Epoxide Ratio Catalyzed by a Fe-Incorporated Octahedra-Based Molecular Sieve. *J. Phys. Chem. C* **2021**, *125*, 13291–13303. [[CrossRef](#)]

Disclaimer/Publisher’s Note: The statements, opinions and data contained in all publications are solely those of the individual author(s) and contributor(s) and not of MDPI and/or the editor(s). MDPI and/or the editor(s) disclaim responsibility for any injury to people or property resulting from any ideas, methods, instructions or products referred to in the content.